

FLEXIBLE MICROFLUIDIC CIRCUIT WITH  
EMBEDDED IN-PLANE VALVE

by

SRIKAR C. PARUCHURI

Presented to the Faculty of the Graduate School of  
The University of Texas at Arlington in Partial Fulfillment  
of the Requirements  
for the Degree of

MASTER OF SCIENCE IN MECHANICAL ENGINEERING

THE UNIVERSITY OF TEXAS AT ARLINGTON

May 2007

Copyright © by Srikar C. Paruchuri 2007

All Rights Reserved

## ACKNOWLEDGEMENTS

I would like to thank my advisor, Dereje Agonafer, for his guidance, support, and for the opportunity he provided. Since summer'05, my work at Automation & Robotics Research Institute (ARRI) has allowed me to learn many new things. I am thankful to my research advisor Dr. Jeongsik Sin from ARRI, for his guidance, support and active involvement in concluding this thesis.

I would like to take this opportunity to express my sincere gratitude to research faculty & my committee members: Dr. Dan Popa, Dr. Woo Ho Lee and Dr. Mason Graff, for their insightful questions and suggestions thorough out my work time at ARRI.

I am thankful to my colleagues Saket and Smitha at MMD Lab, who have helped me to complete my research by taking time to share their lab expertise & providing a stimulating environment with interesting discussions. I would also like to thank Kathleen Elfrink (Admin., ARRI), Sally Thompson (Admin., EMNSPC) and Dona Woodhead (Admin., Department of MAE) for their administrative support through my Master's.

Finally, but most importantly, I would like to extend my deepest thanks to my parents, brother, sister-in-law & other family members for their constant support, encouragement, and confidence in me.

November 27, 2006

## ABSTRACT

### FLEXIBLE MICROFLUIDIC CIRCUIT WITH EMBEDDED IN-PLANE VALVE

Publication No. \_\_\_\_\_

Srikar C. Paruchuri, M.S.

The University of Texas at Arlington, 2007

Supervising Professor: Dereje Agonafer

Recent developments in Microfluidic systems have demonstrated many potential applications related to biology, chemistry and medical sciences. Fluidic manipulation with precise volume control is a basic function in these systems, and microvalves play an important role in control and delivery of the fluid sample. One of the key issues in such valve design is to make large membrane deflections compared to the channel dimension. This thesis reports a flexible microfluidic chip with embedded in-plane valves for fluid manipulation. Silicone elastomer (Polydimethylsiloxane - PDMS) is one of the most suitable materials to fabricate microvalve membranes, because of its low Young's modulus, excellent sealing property and rapid prototyping procedures. The proposed in-plane control valve utilizes pneumatic pressure source to

squeeze the channel and restrict the flow through channel. These in-plane valves can be fabricated in a single layer with a plane top covering layer, hence reduces the multiple layers and alignment issues related to layer stacking. The experimental results show a membrane deflection of  $25\mu\text{m}$  with an applied pressure of 70psi. The prototype valves have a leakage ratio ranging between 0.4 and 0.2. These valves can be used for transportation of continuous and discrete volume flow.

## TABLE OF CONTENTS

ACKNOWLEDGEMENTS.....	iii
ABSTRACT .....	iv
LIST OF ILLUSTRATIONS.....	ix
LIST OF TABLES.....	xii
Chapter	
1. INTRODUCTION.....	1
1.1 Motivation .....	1
1.2 Scope of thesis & Outline.....	2
2. MICROFLUIDICS – OVERVIEW.....	4
2.1 Introduction.....	4
2.2 Microfluidic Systems.....	4
2.3 Benefits of Microfluidics and platforms.....	6
2.4 Challenges & Issues.....	7
2.5 Microfluidics: Market potentials and Applications.....	8
2.6 Microfluidic Components.....	9
2.6.1 Microvalves .....	9
2.6.1.1 Microvalves with external actuation .....	11
2.6.1.2 Microvalves with integrated actuation.....	12
2.6.2 Fluidic Interconnects .....	16

2.7 Conclusion.....	21
3. DESIGN & SIMULATION.....	22
3.1 Introduction.....	22
3.2 Modular Microfluidic Platform.....	22
3.3 Material Selection.....	23
3.4 PDMS Reconfigurable Circuit.....	24
3.5 Microfluidic Components.....	25
3.5.1 Microfluidic Ports & Interconnects .....	25
3.5.2 Embedded In-plane microfluidic valve .....	27
3.6 Simulation of membrane deflection.....	29
3.7 Conclusion.....	33
4. FABRICATION.....	34
4.1. Introduction.....	34
4.2 Fabrication of PDMS based microfluidic circuits .....	34
4.2.1 Mask design & Fabrication.....	34
4.2.2 SU8 Master Mold Fabrication.....	35
4.2.3 Pattern transfer with replica molding.....	40
4.2.4 Fluidic Interconnects & Bonding.....	42
4.3 Conclusion.....	43
5. EXPERIMENTS & RESULTS.....	44
5.1. Introduction.....	44
5.2 Sealing layer and Interconnects Testing .....	45

5.3 Valve diaphragm deflection test .....	49
5.2 Functionality Test.....	51
5.5 Conclusion.....	53
6. CONCLUSION & FUTURE WORK.....	54
6.1. Conclusions.....	54
6.2. Future Work.....	54
Appendix	
A. ANODIC BONDING OF SI & PYREX GLASS DIES.....	55
B. MICRO DRILLING SETUP .....	59
C. EPOXY BASED FLUIDIC INTERCONNECTS .....	62
D. MODIFIED MICROFLUIDIC CIRCUIT DESIGNS .....	64
REFERENCES .....	67
BIOGRAPHICAL INFORMATION.....	72



## LIST OF ILLUSTRATIONS

Figure	Page
1.1 Illustration of microfluidic circuits from <i>Syrris</i> , <i>Epigem</i> and <i>Fluidigm</i> .....	2
2.1 Schematic illustration of modular microfluidic circuit .....	5
2.2 Illustration of Current Microfluidic Market Trend ( <i>Source: IMTEK</i> ).....	9
2.3 Classification of microvalves based on actuation principle. ....	10
2.4 Schematic of microvalves: (a) Cantilever check valve, (b) Piezo actuation based valve, (c) Cantilever type electro static valve, (d) Bimetallic valve, (e) Thermo-pneumatic valve and (f) Electro-magnetic valve configuration.....	14
2.5 Illustration of monolithically fabricated valves. ....	15
2.6 Illustration of latching pneumatic valves .....	15
2.7 Illustration of a capillary pumped system .....	16
2.8 Fabrication process for O-ring couplers.....	17
2.9 Self aligning fluidic interconnects.....	18
2.10 Schematic of PDMS interconnect (a) through-hole type (b) perpendicular type .....	19
2.11 Cross-sectional views of microfluidic test boards and components for (a) fins and (b) notched cylinder/hole interconnects structures.....	20
2.12 Process flows as a demonstration of the concept: (a) discrete processing and (b) integrated processing .....	21
2.13 Schematic of sealing mechanism: (a) discrete and (b) integrated processes.....	21

3.1	Schematic illustration of the Modular Microfluidics .....	23
3.2	Picture of flexible PDMS layer & chip .....	24
3.3	Illustration of chips mounted on top of the platform. ....	25
3.4	Schematic illustration of epoxy based interconnections .....	26
3.5	Illustration of press-fit fluidic interconnects in PDMS .....	27
3.6	Illustration of embedded in-plane microvalve design and its parameters .....	28
3.7	Modeling of diaphragm using ANSYS 9.0: (a) geometry model, (b) free mesh, (c) refined mesh and (d) boundary conditions (displacements & pressure) .....	29
3.8	Maximum deflection of diaphragm with applied pressure (E = 0.75Mpa & 0.36MPa). ....	30
3.9	Deformed shape of the membrane at 70psi with E as 0.75Mpa.....	31
3.10	Von Mises stress of the membrane at 70psi with E as 0.75Mpa.....	31
3.11	Deflected membrane at 70psi with E as 0.36Mpa.....	32
3.12	Von Mises stress of the membrane at 70psi with E as 0.36Mpa.....	32
4.1	Transparency Sheet Printed Mask & Design Layout .....	35
4.2	Developed master molds for different microfluidic circuits .....	39
4.3	Optical profiling of SU8 master mold.....	40
4.4	Before and after degasification of PDMS mixture.....	41
4.5	Transferred pattern on peeled PDMS.....	41
4.6	PDMS Microfluidic chip with fluidic interconnects .....	43
5.1	Die design 233(L = 600 $\mu$ m) & 231(L = 400 $\mu$ m) .....	44
5.2	Photo of experimental setup for pressurizing test .....	46

5.3	Configuration of valve pressurizing test .....	46
5.4	Top view of valve during sealing layer testing (a) valve at 0psi, (b) valve at 80psi and (c) valve at 30psi.....	47
5.5	Trapped gas in a PDMS chip bonded with semi-cured bonding process .....	48
5.6	Testing of PDMS chip bonded with semi-cured bonding process: (a) open valve, (b) single side initiated valve, (c) double side initiated valve, (d) fluid flow before bond failure & (e) fluid flow after bond failure.....	48
5.7	Precession stainless steel interconnects.....	49
5.8	Deflecting valve membrane at various pressures .....	50
5.9	Graphical illustration of <i>deflection Vs pressure</i> .....	51
5.10	Illustration of direction control fluid flow.....	52
5.11	Schematic of leakage testing setup.....	52

## LIST OF TABLES

Table		Page
4.1	Master mold fabrication using photolithography process .....	36
5.1	Change in young's modulus with respect to PDMS mixture ratio.....	50
5.2	Measured flow rate at two peak operating pressures .....	53

## CHAPTER 1

### INTRODUCTION

#### 1.1 Motivation

Research related to integration of MEMS, microfluidics and microoptical components, for microfluidic devices for quick and cost effective sample processing is very demanding. The first microfluidic circuit was a miniaturized gas chromatography system which was created around 1975 [1]. But due to underdeveloped technologies for research in the science community [2] this research area had a recess. In early 90's, with the advancements in the miniaturization has resumed its focus on chromatography application [3], and other applications of microfluidic systems. Since then there were significant number of articles published in journals and conferences. But most of those designs failed to be launched into the market as a product. This is probably because of the complexity in fabrication process, overall cost, fragile materials and compatibility issues related to system design. Later with the use of polymer materials there has been a significant improvement in developing flexible substrates that suite various applications such as microfluidic circuits for polymerize chain reaction (PCR), bio sampling etc. In all these applications the valve plays an important role in controlling the volume and direction.

These issues were the prime concerns through out the research in developing microfluidic circuits with simpler fabrication process with better fluidic control, less

fragile, etc. The figure 1.1 illustrates some of the popular microfluidic analysis products that are available with mass producible future.



Figure 1.1: Illustration of microfluidic circuits from *Syrris*, *Epigem* and *Fluidigm*.

### 1.2 Scope of thesis & Outline

The objective is to develop a low cost flexible & reconfigurable microfluidic circuits for lab based microfluidic handling applications, which involve: developing or using simpler methods for fabrication and characterization of microfluidic circuits; developing components for precise micro/nano/pico liter volume and direction control with fluidic interconnection for fluidic processing.

*Outline:*

*Chapter 2: Microfluidics – Overview* deals with the current state of microfluidics with focus on various aspects such as advantages microfluidics & platform technology, challenges, market potential, and various microfluidic components.

*Chapter 3: Design & Simulation* deals with the design aspects involved in designing different microfluidic circuits with proper material selection, various functionalities

(viz., mixing, multiplexing, dividing...), modular configurations, valves and fluidic interconnects. The in-plane valve simulation using ANSYS, to estimate maximum deflection is also discussed in this chapter.

*Chapter 4: Fabrication* deals with the detailed fabrication process involved in this thesis. It includes different laboratory setups for simplified fabrication. It is divided in to two fabrication approaches implemented based upon material selection.

*Chapter 5: Experiments & Results* is based upon the experiment evaluation of the design and its functionality. The simulation results were compared with the experimental results which are further considered for necessary modifications and future work. The functional verification tests for multiplexing, mixing, modular approach are also explained.

*Chapter 6: Conclusion and Future Work:* This chapter summarizes the achievements from the targeted goals with the results obtained from the initial design and explains the future responsibilities involved in developing a full scale modular microfluidic circuit with increased stability.

## CHAPTER 2

### MICROFLUIDICS - OVERVIEW

#### 2.1 Introduction

This chapter provides an overview of microfluidic systems with emphasis on few selected microfluidic components that are involved in fluid control and interfacing with other components.

#### 2.2. Microfluidic Systems

Miniaturization and MEMS gave birth to microfluidics in the 1990s and today still constitute a large portion of this young discipline [4]. Microfluidics is the term used for many innovative research activities aimed at the development of miniaturized devices/ systems, related to the processing of fluids (liquids and gases) in micro and nano liter scale [5]. The systems that perform various microfluidic operations or involved in the process of micro scale fluid sample processing are called as Microfluidic Systems. These systems can be characterized by their ability in controlling precise & minute volumes of fluid well below the microliter range. In the initial stages of development, a basic microfluidic device/system consists of simple channel geometries that allowed for a few chemical reactions on a glass chip. But current state of microfluidic systems is highly complex, with entire laboratory scaled down to chip level. The increased complexity with various laboratory functional components has induced to identify them as “Lab-on-chip” and “micro Total Analysis System ( $\mu$ -TAS)”



[3]. Depending upon the application, the system behavior & reliability aspect vary. This constitutes to develop various components with respect to the application requirements. Integration of such different components can be done by platform approach, which is also called as microfluidic bread board or circuit board [6, 7]. In the platform approach chips/ components with various functionalities are assembled with the base platform layer with proper interconnect, that enables the integrated microfluidic circuit to perform as a complex system for example Micro-TAS. The complexity of the system can be further increased by integrating some active function in the based platform layer, by which it can behave as an active platform base platform can also. The figure 2.1 illustrates a modular microfluidic circuit with platform approach.

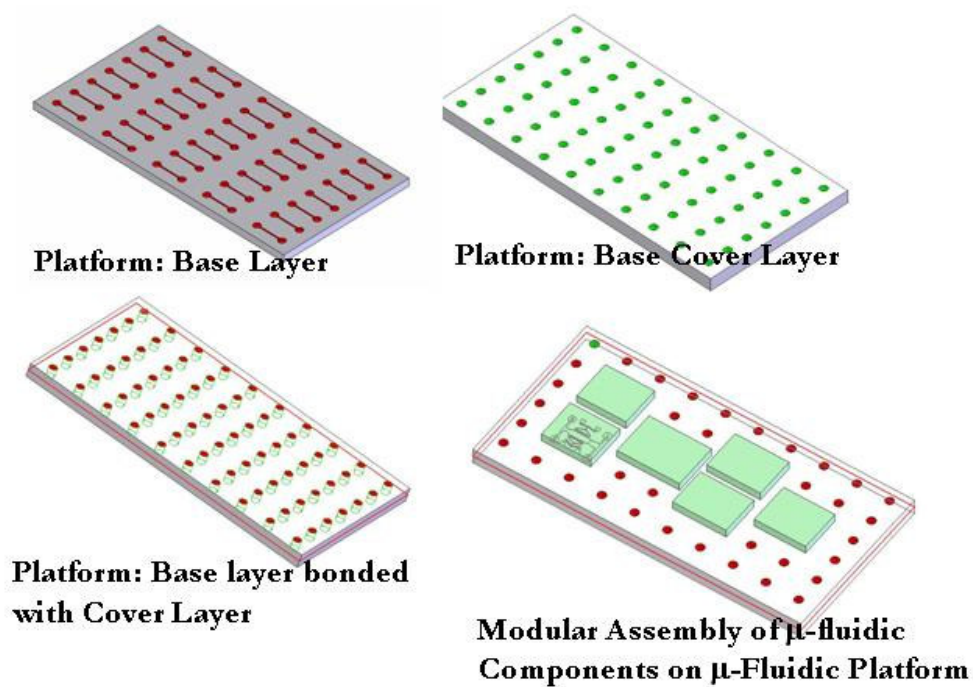


Figure 2.1: Schematic illustration of modular microfluidic circuit.

### 2.3 Benefits of Microfluidics and platforms

The benefits of microfluidic platforms are as follows:

- Low consumption of chemicals and less waste: From the fact about the micro and nano scale fluid handling, the overall consumption of reagents and test samples in an analysis is drastically reduced. This leads to reduce in cost for expensive reagents and reduced amount of waste. .
- Enhancement of analytical performance: The enclosed environment of most microfluidic devices can be easily controlled due to very limited exchanges with the ambient is allowed.
- Low power budget: The small size of microfluidic devices enables portable systems if the power requirements of the detection schemes employed are sufficiently low.
- Low-cost fabrication and packaging: With improved system design the overall cost in fabrication and packaging is low
- Platforms with lab on chip capabilities will reduce over all time, cost in analysis and also possible errors that are caused due to frequent sample handling during the process.
- Portable analysis system: A cheap and disposable microfluidic platform is useful in conducting analysis at remote locations where laboratories are at distant.

- Reconfigurable Circuit: A reconfigurable circuit is used to perform different tasks by varying the circuit configurations. For example: mixing, multiplexing, separation etc.

#### 2.4 Challenges and Issues

Issues and challenges related to the behavior of the fluid and system:

- Viscous Dissipation Effect (temperature, pressure and velocity): When the flow channel dimensions are nearing to the micro level then viscous dissipation effect is significant. It leads to change in velocity gradient near the walls, increases the temperature near the wall and hence the viscosity (Function of temperature) also varies resulting the pressure variation and Reynolds number variation. [8].
- Reynolds number: Due to lower Reynolds number the flow in channels is laminar. This will not help in mixing two fluids. In this case diffusion is the only method to implement in helping the mixing. The mixing through diffusion requires long channels. This can be a draw back if the channel lengths are small.
- Capillary Forces (due to surface tension): Large capillary forces are generated due to small a channel spreads the fluid through unwanted portions of the system and leads to increased contamination.
- Surface Roughness Effects: The pressure gradient and flow friction are higher than those from conventional laminar flow theory [9]. This can be considered as an effect due to surface roughness.

- Clogging and Blocking: Clogging is severe adhesion of the molecules of liquids, gases, and dissolved substances to the surfaces of solids over a long period of time, and may cause bottlenecks and even blocking of channels.
- Pressure drop and dead volume due to differential geometries at channels, valves, pumps and interconnects and due to miscibility, viscosity, or binding energy
- Packaging: Developing a reliable packaging process for polymer based and silicon based microfluidic systems which involve fluidic and electric connections is tricky.

### 2.5 Microfluidics: Market potentials and Applications

Microfluidics has developed steadily over the past few decades with the development in fabrication, testing & modeling techniques. The first commercial applications were in the field of printing technology, where ink-jet printer head required controlled dispensing of Pico liter to Nano liter amount of ink while printing. The motivation developed from microscopic analysis, biodefence, & microelectronics allowed it to spread in to various application areas. Companies such as Micronics Inc. with active lab cards, Fluidigm® with multi layer microfluidics, ThinXXS with microfluidic tool kits, and Cellix Ltd with bio-chips, and others have proven their ability to mass produce latest products such as Lab-On-Chips, and customer specific microfluidic systems. From the below classification (figure 2.1) it can be understood that major part of research and development is under Life Sciences.

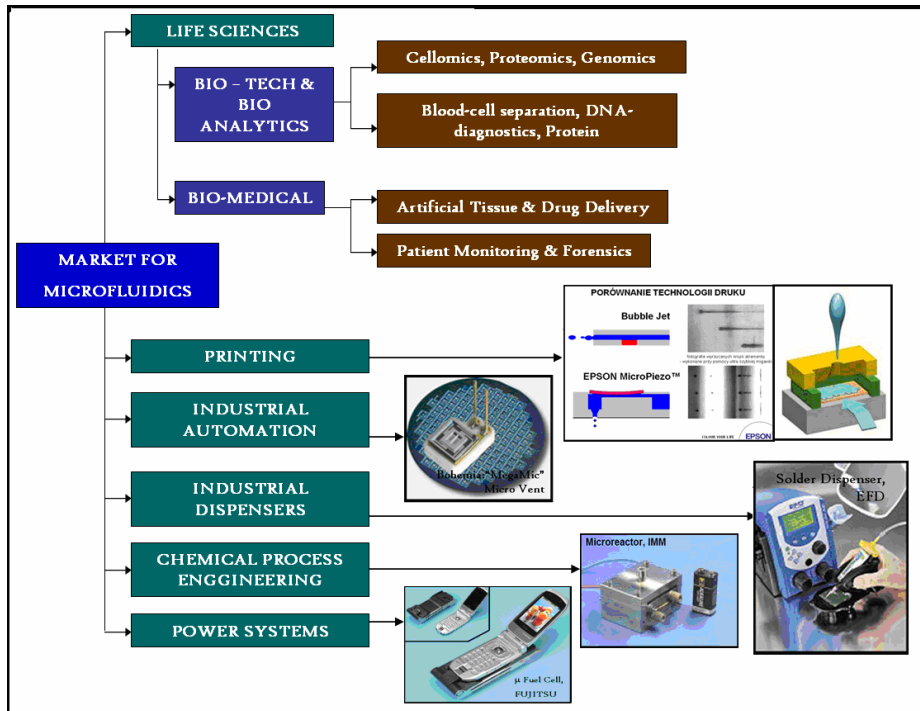


Figure 2.2: Illustration of Current Microfluidic Market Trend (Source: IMTEK).

According to market studies, the microfluidic market for life science applications reached \$350 million in 2004 (source: Yole Development Market Research) and is projected to grow to \$2 billion by 2010.

## 2.6 Microfluidic Components

The most important components of any microfluidic systems are microchannels, micropumps and valves, micromixers (Active and Passive), microsensors, reservoirs and fluidic interconnects. Depending upon the system functionality their configuration varies.

### 2.6.1 Microvalves

Microvalve is a controlling component with multi-functional capabilities such as fluid flow rectification, direction control through the circuit, input and output control

can be performed. The conventional valves used to control the pressure and flow, typically use magnetic actuation in the form of solenoids or motors to drive diaphragms or spool valves. There are many ways to categorize microvalves viz., based upon the configuration (open and closed), control pattern (analog and digital), based upon actuation principles. It is feasible to categorize them based upon actuation principle which introduces to various mechanisms and materials. Based upon the actuation the microvalves can be sub-divided in two classes, *active microvalves* and *passive or check valves*. The passive/ check valves are those which don't have any actuation mechanism. They operated upon the pressure difference across the valve. The figure 2.4.(a) illustrated a simple configuration of a cantilever type silicon based check valve. The active microvalves require energy to operate and can be further classified based upon their actuation mode, external actuators & integrated actuators [9]. The classification of microvalves based upon actuation method is illustrated with figure 2.3., followed by their definitions.

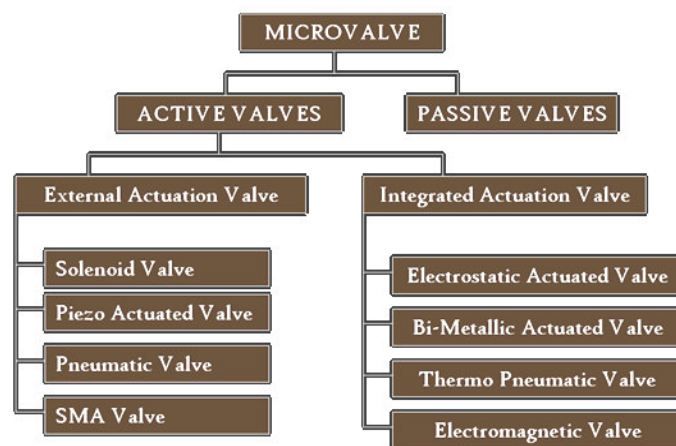


Figure 2.3: Classification of microvalves based on actuation principle.

#### *2.6.1.1. Microvalves with external actuation*

The valves that fall under this section are *solenoid, piezoelectric, pneumatic* and *shape memory alloy* actuated valves.

The ***solenoid plunger valve***, utilizes the electromagnetic actuation principle. The valve performance with this technique depends upon the applied current that drives the actuator and number of coil turns through the solenoid. External solenoid actuators were used with good success in the earlier version of the integrated gas chromatograph [10]. Integration of such a valve is difficult because of the difficulties in achieving significant number of turns in a solenoid, low-loss magnetic return path and larger area to accommodate the system.

***Piezoelectric actuators*** are commercially available in the form of disks and cantilever beams. These are bimorph based valve arrangements with relatively larger deflections from the beams, but poor corresponding force. The displacement from a stack of these actuators is comparatively very large with smaller strokes. Hence the stack has very low response time. This valve arrangement is illustrated in the figure 2.4(b).

***Pneumatic actuated valve*** utilizes an external pneumatic source with a source controlling valve and a pressures source that drive the actuators based upon the external pneumatic valve controlling. The force and displacements in this method can be controlled with a wide range. The response time for this method depends upon the flow conductance through the tubing connected through the external valve & micromachined elements. The size of the micromachined components can be quite small, but

miniaturizing of the external valves is difficult. Based upon this actuation method, a polymer embedded in-plane valve has been developed and is discussed in the later chapters.

*Shape memory alloy actuation* based actuators are metal strips/ coils that can remember their initial shape before deformation and regains its original shape by itself normally or during heating at higher ambient temperatures. The three main types of SMA are the copper-zinc-aluminum, copper-aluminum-nickel, and nickel-titanium (NiTi) alloys. NiTi alloys are more expensive and possess superior mechanical properties when compared to copper-based SMAs during unloading. A pressure of about 0.2Mpa (30psi) and a displacement of about 1mm can be achieved from a Ti-Ni 3mm wounded coil with a wire diameter of 0.5mm [11]. This approach is best suitable for on/off applications because it is difficult to control the displacement, with this it fails to satisfy the need of precise flow controlling.

#### *2.6.1.2. Microvalves with integrated actuation*

The valves that fall under this section are electrostatic valve, bimetallic actuated valve, thermo-pneumatic actuated valve and electro-magnetic actuated valve [10].

The simple arrangement of an *Electrostatic actuation* based valve shown in figure 2.4(c), consists of movable planar electrode and a fixed electrode. Large gap between the electrodes cause less force. The controllable pressure range with this mechanics is also limited. The fluid pressure is used to further enhance this valve operation with wider opening [12].



A *Bimetallic actuation* based valve can generate strong forces and reasonable displacement with proper selection of the two materials. The pressure generated is directly proportional to the difference between the thermal expansion coefficients of the two materials and temperature difference. The silicon diaphragm with an aluminum layer is most popular combination observed in this section. The figure 2.4(d) illustrates the operation and cross section of a simple silicon & aluminum based bimetallic valve arrangement.

The *thermopneumatic* valve is equipped with a sealed pressure chamber and a movable diaphragm. The valve arrangement observed in figure 2.4(e) is based upon thermal expansion of a thin layer of paraffin wax [16]. When the actuator is activated, by heating the fluid in the chamber which expands and diaphragm deflects vertically by pressing the thin diaphragm layer against the valve seat thus sealing the outlet hole. Since paraffin can provide very large actuation forces, a very good seal is easily attained with low actuation power.

The electromagnetic valve configuration with a valve cap made of Ni-Fe alloy, supported by a spring is observed in the figure 2.4(f). The magnetic field produced from the external electro magnet allows it to move vertically. This valve was designed to regulate the flow for high vacuum application [17], which is operated between  $3 \times 10^{-5}$  torr-liter/min to  $2.4 \times 10^{-3}$  torr-liter/min at a pressure of  $4.6 \times 10^{-7}$  torr. This type of microvalve can be mounted inside a small tube with an external coil mounted outside the tube.

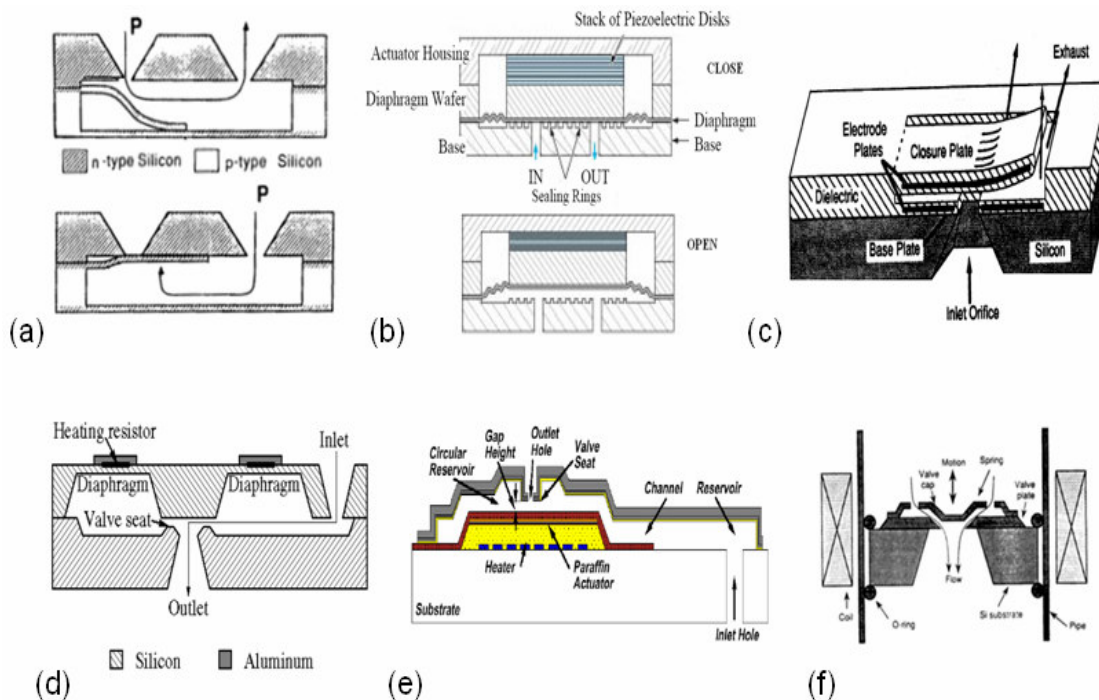


Figure 2.4: Schematic of microvalves: (a) Cantilever check valve, (b) Piezo actuation based valve [12], (c) Cantilever type electro static valve [14], (d) Bimetallic valve [15], (e) Thermo-pneumatic valve [16] and (f) Electro-magnetic valve configuration.

The following are some of the most popular designs in valving which are highly inspiring in development of microfluidic platforms in polymer material with complex fluidic circuits and matrix valve arrangements to control the fluid through those circuits:

The monolithic microfabricated valve by Marc A. Unger, et al, [18] explains the fabrication technique and approach involved in developing a soft and flexible channel and valving approach. This technique is most widely used with minor modifications in many designs. One such similarity can be observed in [7], where the channels are squeezed to perform the valving. These are normally open type. They can be closed by supplying the pneumatic pressure through the valve inlet line. The figure 2.5 illustrates

a fluid channel which can be operated as open and close arrangements and also can be operated for peristaltic pumping by supplying the pressure through the valve channel.

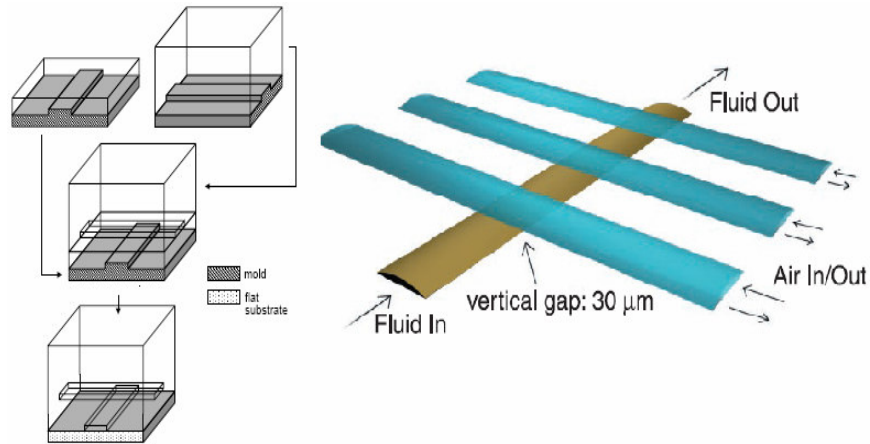


Figure 2.5: Illustration of monolithically fabricated valves [18].

The novel latching microfluidic valves by William HG., et al [19], are based on pneumatic monolithic membrane valves, with normally closed stage and operated with a vacuum for opening and closing. The valve control unit is connected with two additional valves, a valve responsible for holding the latching valve open by and with other pressure line to close the opened valve [19]. The figure 2.6 below illustrates the valve design and operation.

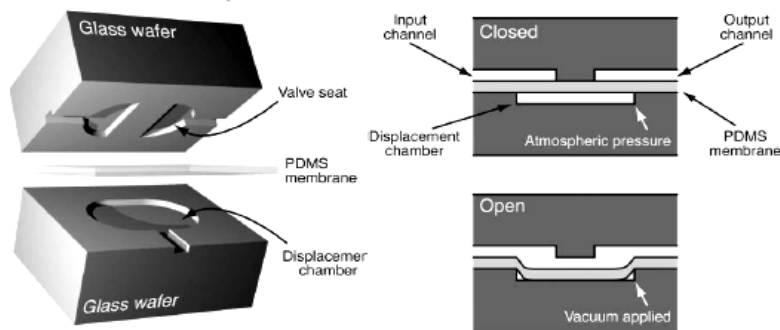


Figure 2.6: Illustration of latching pneumatic valves [19].

The capillary pumped microfluidic system developed by [20], utilizes a capillary pumping action that closes the channel as observed in figure 2.6. The arrangement of this system, such that the plunger when turned on squeezes the channel and when it is turned off it retracts back with the elasticity of the material.

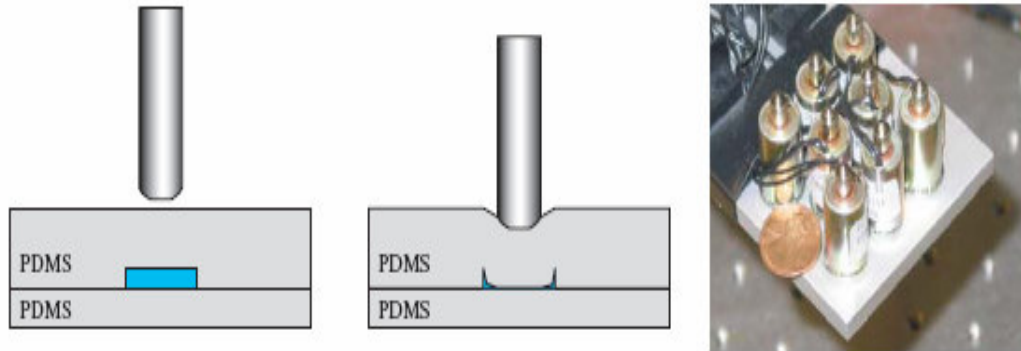


Figure 2.7: Illustration of a capillary pumped system [20].

### 2.6.2 Fluidic Interconnects

Due to expansion in field of microfluidics with the technology that lead to development of many fluid handling components such as micropumps, microvalves, micromixers etc which are assembled to demonstrate a microfluidic system that can perform various tasks such as micro-TAS. If these systems are not properly connected to the outer world, it would be of no use in developing such a system. To satisfy the need, we need proper fluidic interconnects that provide coupling in-between microfluidic circuits or between the microfluidic circuit and the outer world. The selected overview of simple interconnection techniques from [21] helps in understanding the currently available techniques and also allows us to improve reliable design depending upon the system requirements.

Tze-Jung Yao [22] presented a novel technique called “quickconnect” for microfluidic devices with a simple silicone-rubber O-ring MEMS coupler. The O-ring couplers are easy to fabricate and utilize, reusable, can withstand high pressure (>60psi), and provide good seals. In their paper, results from both the leak rate test and pull-out test are presented, demonstrating the functionality of the O-ring couplers. The figure 2.8 illustrates the bonding mechanism involved in this paper.

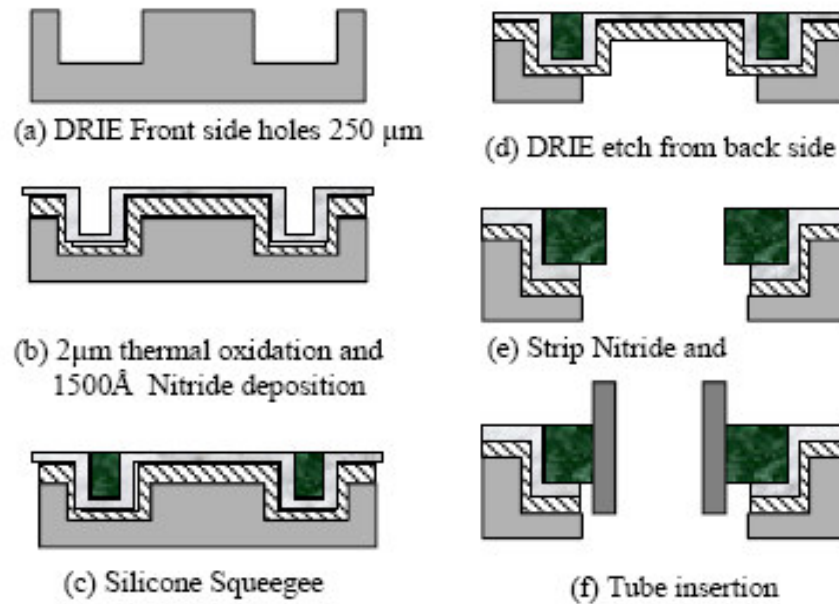


Figure 2.8: Fabrication process for O-ring couplers [22].

Puntambekar A. et al presented a novel self-aligning fluidic interconnection technique with low dead volume and pressure drop for generic microfluidic systems [23]. The design, fabrication and characterization of the two self-aligning fluidic interconnections were explained. The first technique was a serial assembly technique, in which each fluidic interconnect is assembled individually, exhibiting a pressure drop of 977Pa (0.14psi) at a flow rate of 100 $\mu$ l/min. The second technique was based upon

parallel assembly technique that is suitable for high-density interconnects with multi-stacked generic microfluidic systems, which has a pressure drop of 1024Pa (0.15psi) at a flow rate of 100 $\mu$ l/min. They also simulated the flow characteristics of these interconnection schemes and, based on the simulation results, designed the above interconnection schemes. The serial interconnection scheme could theoretically withstand 2.6MPa and the parallel interconnection scheme could withstand a theoretical maximum pressure of 6.6MPa. Figure 2.9 illustrates the technique implemented.

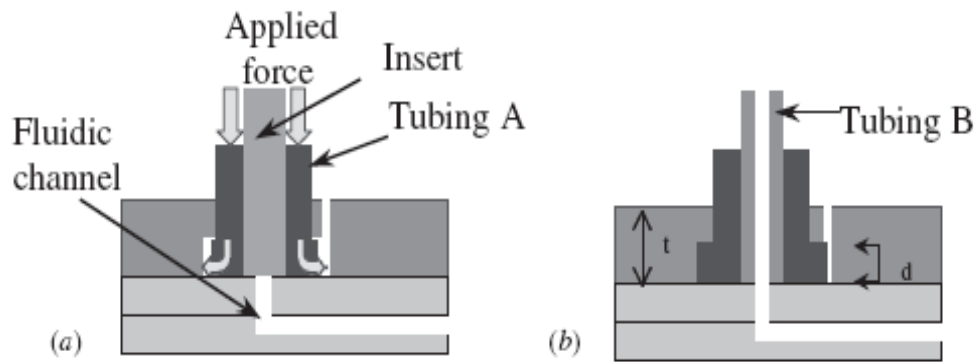


Figure 2.9: Self-aligning fluidic interconnects [23].

Li & Chen in [24] demonstrated the use of Polydimethylsiloxane (PDMS) for interconnections. They used two types of interconnection approaches, one approach was based on through hole and other was on perpendicular type. The interconnections formed were capable enough to handle pressure up to 530KPa. The figure 2.10 illustrates the designs.

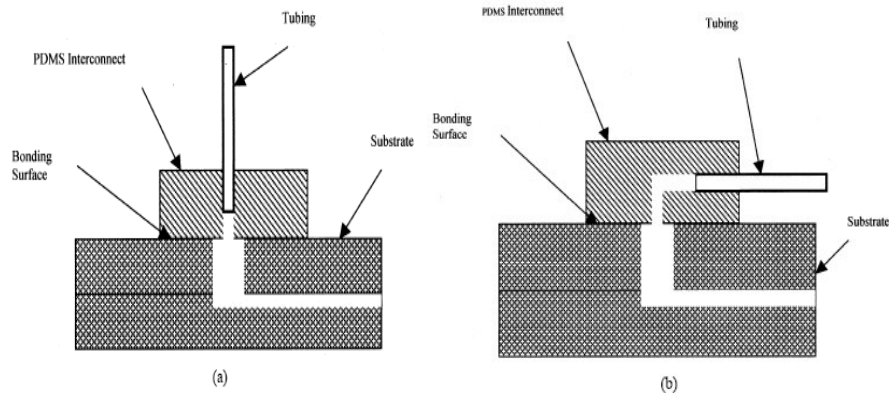


Figure 2.10: Schematic of PDMS interconnects (a) through-hole type and (b) perpendicular type [24].

Gray B. L. [25] et al., developed an interconnection technique using deep reactive ion etching (DRIE) process. The DRIE approach is used to fabricate mechanically interlocking structures through which high-density fluidic interconnections were provided between substrates. The geometric flexibility that can be achieved with DRIE process facilitated the fabrication of high density interconnects of two types: (a) structures with mechanically interlocking “fins” used to align arbitrarily placed fluidic via holes and (b) interlocking hole and notched cylinder pairs that accomplish mechanical and fluidic interconnect in the same structure. Both the interconnects were tested with a silicon microfluidic circuit boards with off-chip coupling for flow control and measurement, and components that consist of simple channel arrays, up to pressures of 100KPa and 70KPa. Figure 2.11 illustrates the designs.

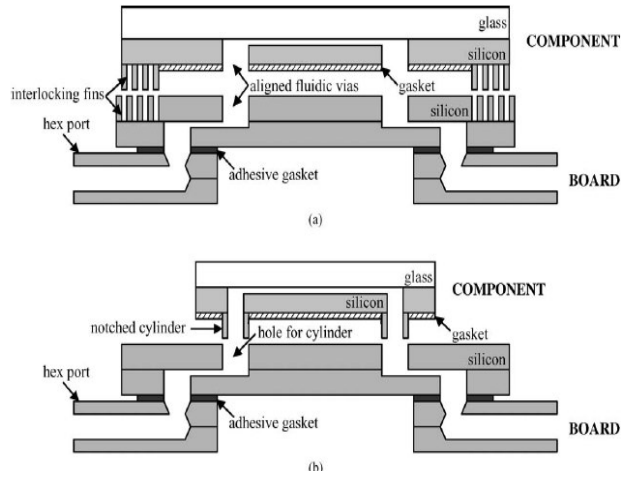


Figure 2.11: Cross-sectional views of microfluidic test boards and components for (a) fins and (b) notched cylinder/hole interconnects structures [25].

Jr. Hung Tsai, et al in their work [26], designed, fabricated and tested interconnects with polymer sealant (Mylar) insertion between the tubing and the fluidic port. Discrete and integrated Mylar sealant processes were developed by means of post-fabrication after the microfluidic components. Microfabrication techniques were utilized during integrate process to facilitate the batch processing with precise control over the sealant. In both (discrete and integrated) processes, capillary tubes with a diameter of  $320\mu\text{m}$  were been successfully connected to microscale channels with the help of the Mylar. Leakage and pull-out tests were conducted and successfully demonstrated the functionality of the interconnections. The leakage test showed that no leakage is observed up to 190KPa and the pull-out test proves 100% survival rate under a pulling force of 2 N. Figure 2.12 (a,b) illustrates the process implemented and figure 2.13 with schematic of sealing mechanism in (a) discrete and (b) integrated processes



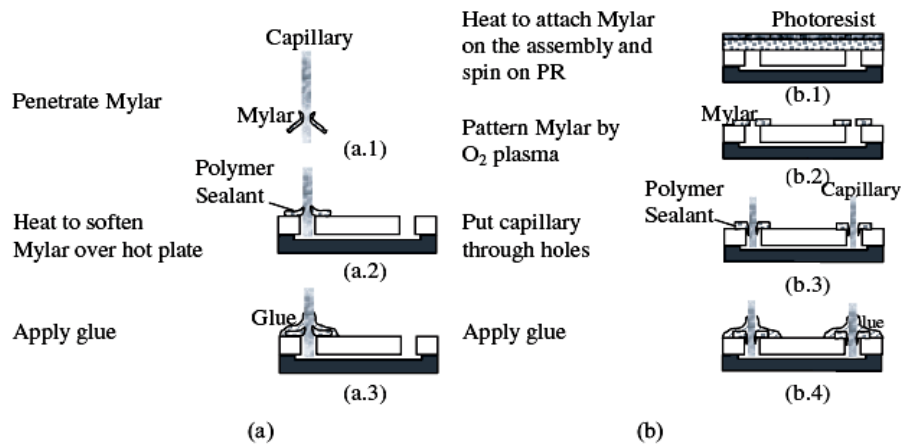


Figure 2.12: Process flows as a demonstration of the concept: (a) discrete processing and (b) integrated processing [26].

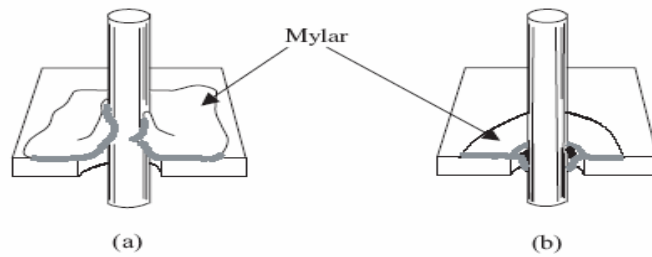


Figure 2.13 Schematic of sealing mechanism: (a) discrete and (b) integrated processes [26].

## 2.7 Conclusion

Hence from this review about the microfluidic systems and its components such as microvalves and interconnections, it is clear that lot of work has been done in order to develop reliable systems for fluidic handling. With the knowledge from this review, simple techniques implemented and developed to produce microfluidic circuits are explained in the following chapters.

## CHAPTER 3

### DESIGN & SIMULATION

#### 3.1 Introduction

In this chapter, the design process involved in microfluidic circuits for modular microfluidics platform is explained. The design concept of modular microfluidic platforms and components integration is also highlighted in this chapter. The components can be a microfluidic circuit/ chip or various microfluidic components that can be mounted on the platform

#### 3.2 Modular Microfluidic Platform

The idea of microfluidic platform is derived from a breadboard, which is reusable device and used to build various prototype systems for experimenting purpose by integrating different components. Similar approach followed by integration of MEMS and Microfluidic Components/ Devices/ Circuits to develop a prototype system for various microfluidic applications. The design of this platform involves integration of the microfluidic circuits with a function of microfluidic manipulation on a fluidic platform.

The design process for the microfluidic platform and circuits are material selection, dimensions, actuation principle, functions, & fabrication process. The Figure 3.1 below gives a schematic illustration of a modular microfluidic platform design with integration of various components such as mixing, controlling, flow extending, etc.

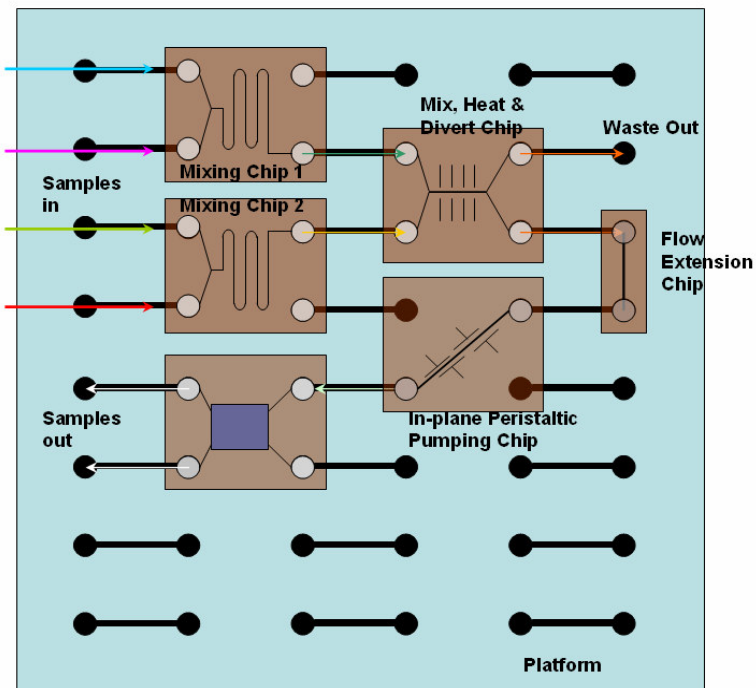


Figure 3.1: Schematic illustration of the Modular Microfluidics.

### 3.3 Material Selection

Material selection is an important stage in any system design. It affects the system's geometry, actuation principles for movable parts, physical application, and reliability. To avoid these issues proper material selection is required. At first, Silicon with Pyrex glass cover was considered to fabricate these modular microfluidic systems and its components. But due to the issues related to lengthy fabrication process, handling and cost, provided the need to modify the material. The material chosen to fabricate the Microfluidic circuits was Poly Di Methyl Siloxane (PDMS). PDMS polymer has numerous advantages over silicon and glass. It is inexpensive, flexible, and optically transparent down to 230 nm (compatible with many optical methods for detection) and also bio and chemical compatible in most cases [27]. Other major

advantages of PDMS are rapid prototyping and ease in bonding with silicon over Pyrex [27]. As PDMS is very cheap and easy to fabricate, it allows us to mass produce the Microfluidic circuits with a well suited process. By varying the mixture ratios, soft and flexible chips can be fabricated. The figure below illustrates the flexibility of a PDMS Layer of 10:1 ratio mixture.



Figure 3.2: Picture of flexible PDMS layer & chip.

### 3.4 PDMS Reconfigurable Circuit

The dimension of a system plays an important role in defining the system. The current trend towards integrating multiple functions in a single system is rapidly increasing. Satisfying the need of integration of active functions like pumping, separation, & manipulation in single chip introduces complex circuits, with lengthy fabrication approaches and more prone to system failure. Hence, chip with unique function, can be mounted on the platform as shown in figure 3.1 to perform a sequence of operations as a single system. With this approach, the platform with different chips like mixing, diversion, multiplexing, pumping, heating etc., can be used to perform various operations on a single platform. The figure 3.3 below gives the schematic

illustration of the assembled chips with various functions. These chips are mounted on top of the platform with a suitable port array to maintain the fluid flow and to manipulate the fluid from one chip to another chip. To make is more flexible architecture, the arrangement can be either modified with the design of the channels and port position, or by using *extension chips* which consists of just straight channels.

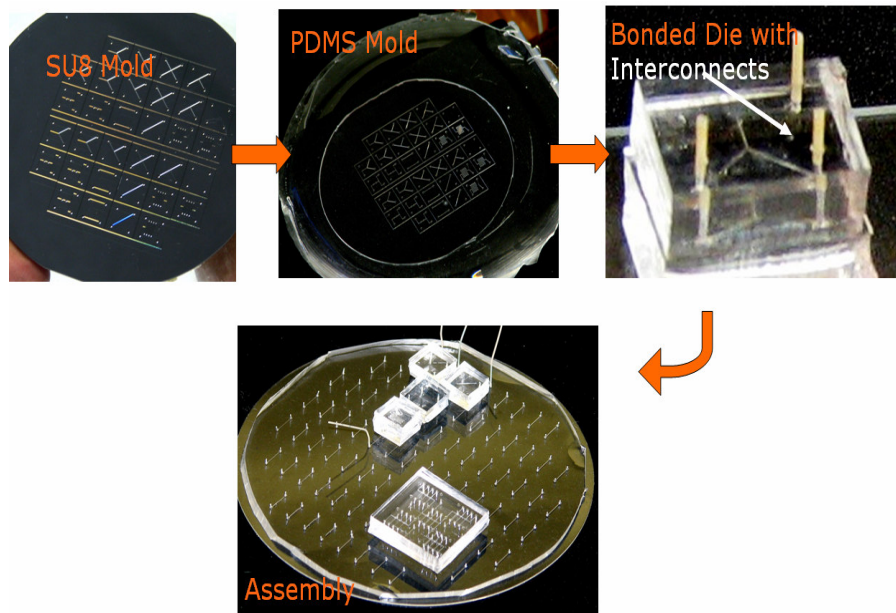


Figure 3.3: Illustration of chips mounted on top of the platform.

### 3.5 Microfluidic Components

In this section we discuss about the design of microfluidic components (microfluidic interconnects and valves) that facilitate fluidic manipulation.

#### *3.5.1 Microfluidic Ports & Interconnects*

The ports and interconnections help in fluid exchange between the system and outer world. Integrated on chip fluidic connections between the micro-scale device and ‘macro-scale’ tubing have been proposed in this section.

The type of fluidic interconnects and fabrication approaches differ with the chip material properties. The fluidic interconnects for a silicon based chips are provided with the helps of epoxy based technique. First ports are drilled with a micro drilling setup and then the capillary interconnects are glued to the substrate with the help of an epoxy. For easier alignment, less epoxy leakage in to channel, the fluidic interconnects for silicon were provided with support tubing. Initially the capillary tube is glued with surrounding external tube which is smaller in length, and with tight tolerance between the capillary and support tube. Later the capillary tube with support tube is inserted in to the drilled port and then glued using of epoxy. The figure 3.4 gives a schematic illustration of the cross section of the epoxy based fluidic interconnects. The detailed fabrication procedure is explained in appendix.

The fluidic ports for a PDMS substrate are made using of a punch tool and then a press fit interconnection is provided by using capillary tube with larger outer diameter than the punched port as illustrated in figure 3.5. The detailed fabrication procedure for this method is provided in chapter 4: Fabrication.

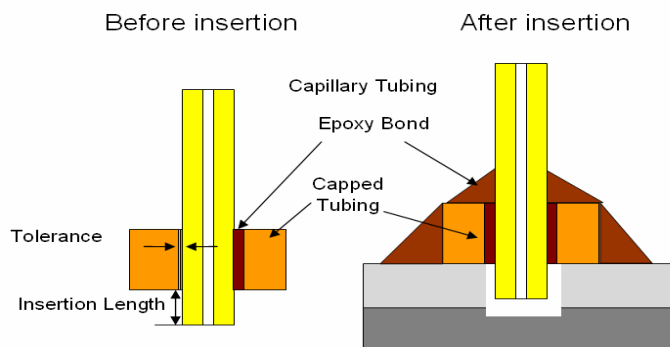


Figure 3.4: Schematic illustration of epoxy based interconnections.

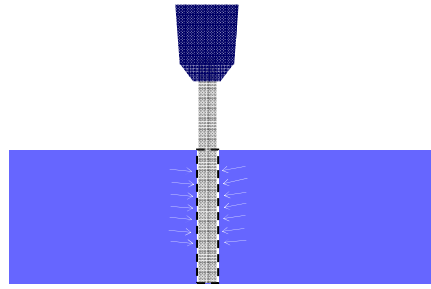


Figure 3.5: Illustration of press-fit fluidic interconnects in PDMS.

### 3.5.2 Embedded In-plane Microfluidic Valve

Microvalves are essential components in many microfluidic systems with potential applications related to biology, chemistry and medical sciences. Valving is often used in these systems for precision volume control and manipulation. For this embedded valve designs, the material chosen for the membrane often must be capable of large deflections relative to the channel dimensions [28]. The silicone elastomer, PDMS, is one of the most suitable and well recognized materials to fabricate such microvalve membranes because of its low Young's modulus and excellent sealing properties [29]. The in-plane control valve is a thin membrane structure that makes up one wall of the flow channel. A pneumatic pressure is used to deflect the membrane into the channel, thereby restricting the flow through channel. The major advantage of in-plane valve is in single layer fabrication technique. This provides reduced number of layers and alignment issues related to layer stacking that are observed in fabricating vertical valve structures, hence it allows easier and quicker fabrication of the microfluidic system. A microfluidic chip with embedded in-plane valve is shown in figure 3.6. The design parameters of developing the thin membrane valve are:

w - Channel width;

L - Length of the membrane;

a - Bonded membrane area with the top sealing layer;

$t_z$  - Height of the membrane.

The device fabrication process involved is explained in under *Fabrication of PDMS based Microfluidic Circuits* in chapter 4. ANSYS Simulation is performed to determine the deflection of the valve membrane which can be observed in the following section. The experimental evaluation and results for the valve deflection are explained in chapter 5.

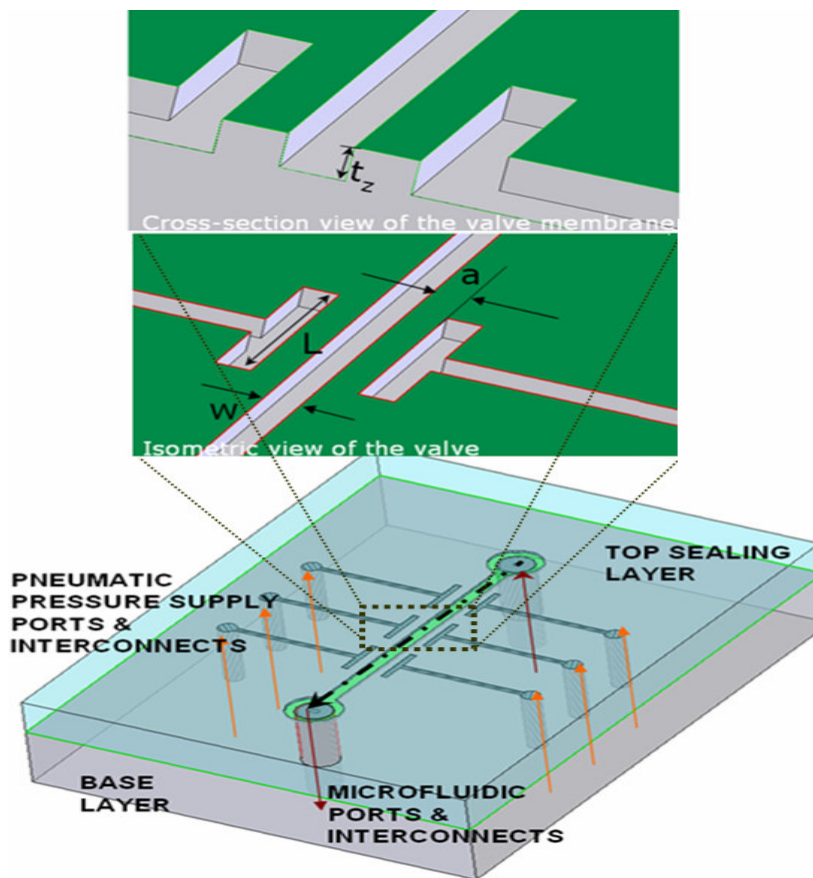


Figure 3.6: Illustration of embedded in-plane microvalve design and its parameters.



### 3.6 Simulation of membrane deflection

This section introduces the simulation of the membrane to guide the valve structure design.

The valve membrane is considered as a thin wall with displacement constraints through out the peripheral of the membrane. The element type used to model the geometry is a 10 node tetrahedron 3D SOLID 92. The SOLID 92 elements have quadratic displacement behavior and they are well suited to model irregular meshes. This element type is defined by ten nodes having three degrees of freedom at each node: translations in the nodal x, y, and z directions. This allows us model the PDMS rectangular diaphragm easily. A rectangular diaphragm was modeled as in figure 3.7(a) with length 600 $\mu\text{m}$  (length), height 100 $\mu\text{m}$ , and thickness of 80 $\mu\text{m}$ . The initial meshing is performed by free mesh option as seen in figure 3.7(b) and then refine at all as shown in figure 3.7 (c). The block is fully constrained at the peripheral as seen in figure 3.7(c).

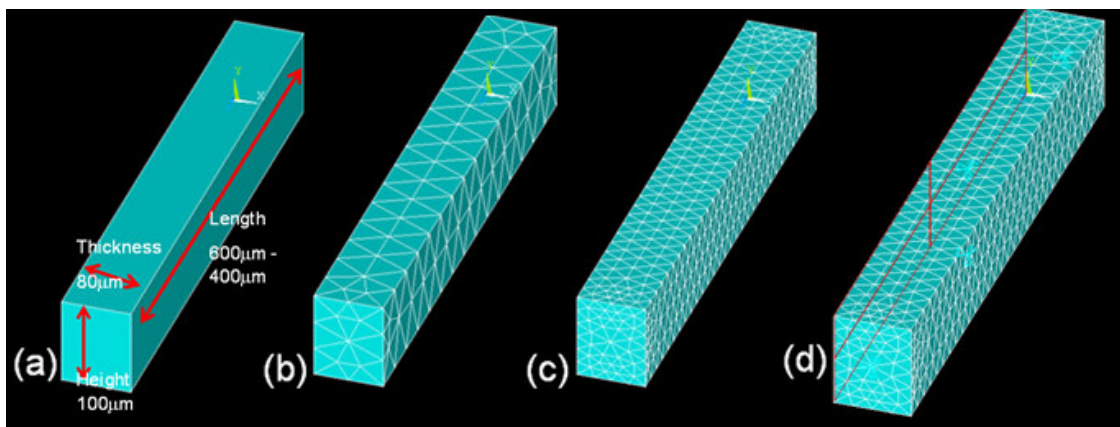


Figure 3.7: Modeling of diaphragm using ANSYS 9.0: (a) geometry model, (b) free mesh, (c) refined mesh and (d) boundary conditions (displacements & pressure).

The pneumatic actuation pressure ranging from 0psi to 80psi is applied on one side of the block as seen figure 3.7(d). The figure 3.8 gives the maximum deflection for applied pressure. The PDMS with low young's modulus of 0.36Mpa with 15:1 mixture ratio [30] is also simulated and the resulting deflections for this can be observed in figure 3.8.

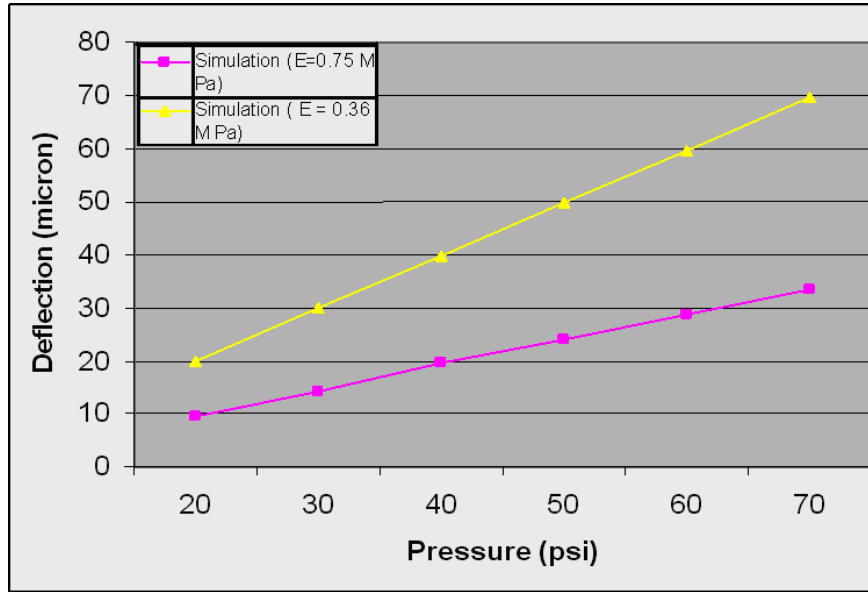


Figure 3.8: Maximum deflection of diaphragm with applied pressure (E = 0.75Mpa & 0.36MPa).

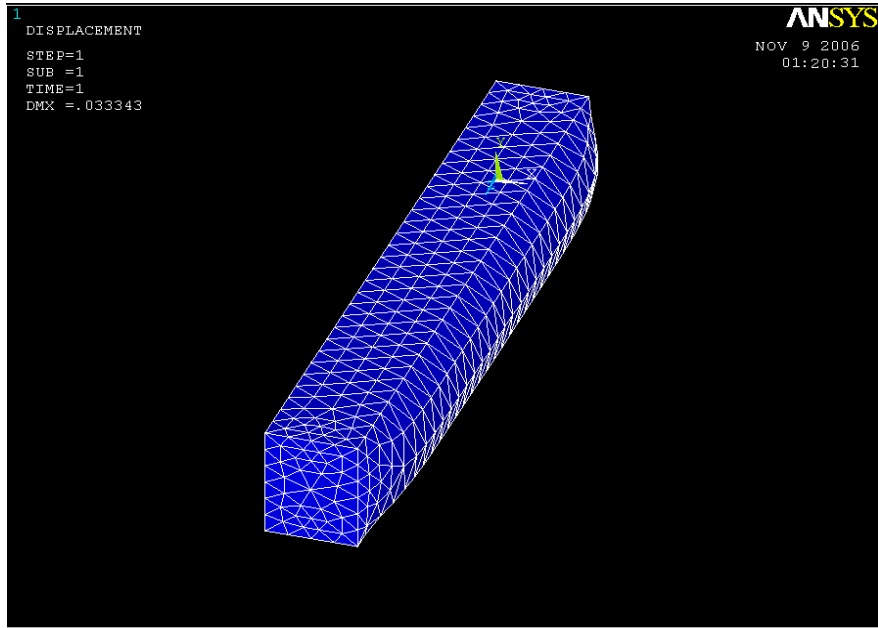


Figure 3.9: Deformed shape of the membrane at 70psi with E as 0.75Mpa.

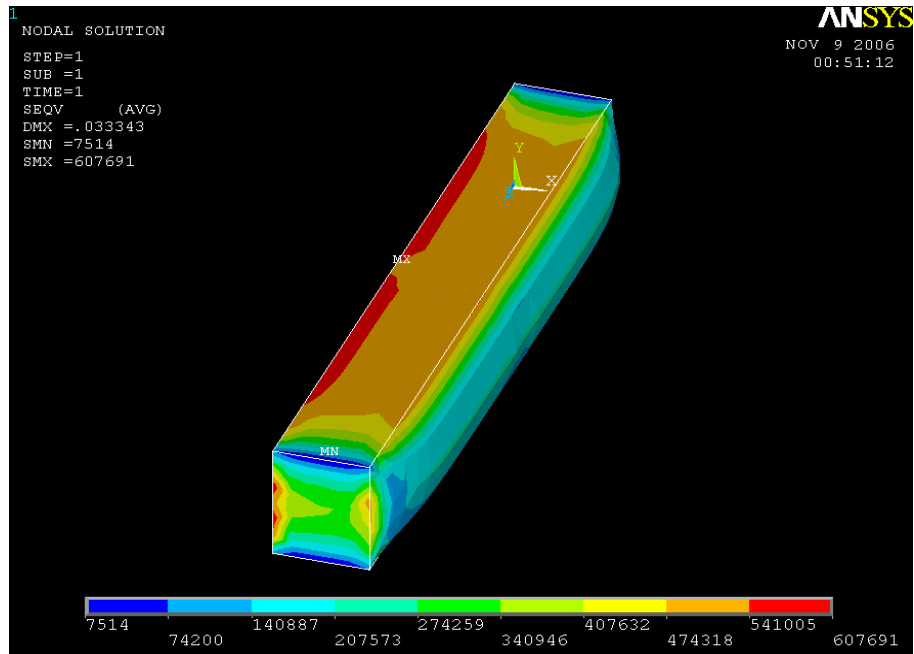


Figure 3.10: Von Mises stress of the membrane at 70psi with E as 0.75Mpa.

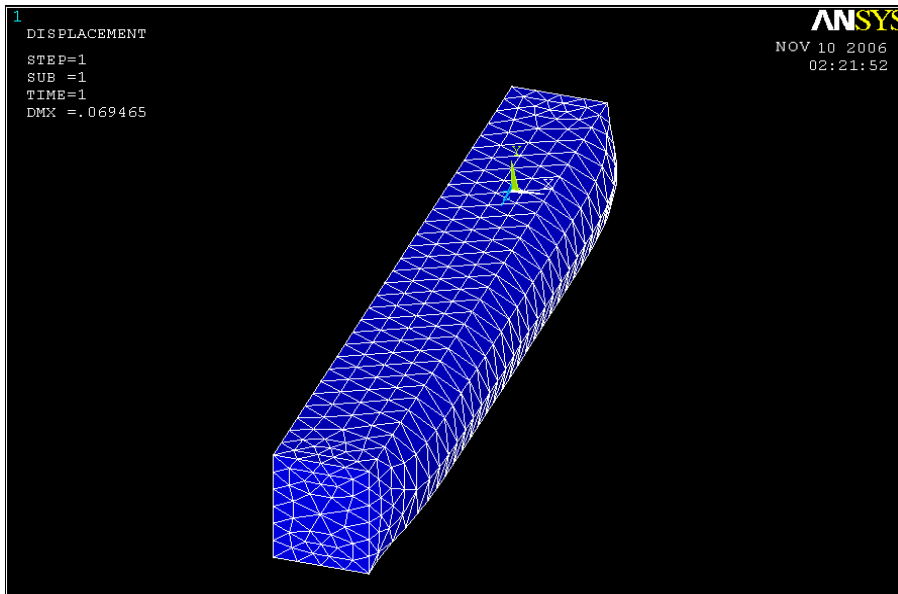


Figure 3.11: Deflected membrane at 70psi with E as 0.36Mpa.

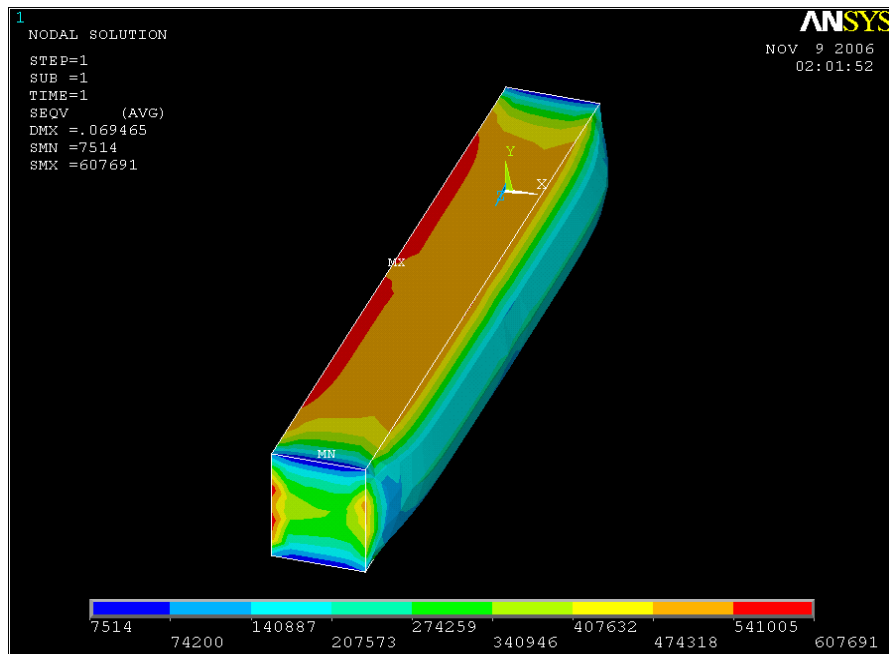


Figure 3.12: Von Mises stress of the membrane at 70psi with E as 0.36Mpa.

From the above figures (3.8 – 3.12) it is clear that the maximum deflection at maximum pressure 70psi for young's modulus 0.75MPa is 33.34  $\mu\text{m}$  and with a young's modulus of 0.36MPa is 69.46  $\mu\text{m}$ .

### 3.7 Conclusion

A design of microfluidic circuit was proposed to provide embedded in-plane valve arrangement with fluidic interconnections. The simulation results showed that the maximum deflection for a 600 $\mu\text{m}$  & 400 $\mu\text{m}$  length diaphragm were 33.33 $\mu\text{m}$  and 69.54 $\mu\text{m}$  respectively. The verification of this design is done by fabrication and experimental evaluation of the valve and interconnects.

## CHAPTER 4

### FABRICATION

#### 4.1 Introduction

Building a microfluidic circuits involve fabrication of open channels, sealing of open channels and fluidic interconnections. The process implemented to fabricate varies with respect to the material used. This chapter explains the fabrication process to fabricate the PDMS Microfluidic circuits presented in earlier design chapter. The fabrication of silicon based microfluidic circuits are detailed in the appendix.

#### 4.2 Fabrication of PDMS based microfluidic circuits

The fabrication of PDMS based microfluidic circuits are performed by Soft Lithography technique. Soft lithography can be defined as a method for fabricating or replicating structures using elastomeric stamps, molds, and conformable photomasks [31]. This process involves:

- Mask Design & Fabrication
- Fabrication of SU8 Master Mold (Photolithography)
- Pattern transferring with PDMS Casting
- Fluidic Ports & Bonding/ Sealing

##### *4.2.1 Mask Design & Fabrication*

Masks are generally used in photolithography process to transfer the pattern on to photoresist and develop the patterns on the substrate. There are various tools available to design a mask; in our case we used LASI and Auto CAD to design the

mask. Mask printing technique and material is varied based upon the feature size & required resolution. But in most cases with feature size up to 10 micron resolution, transparency sheet masks will work fine if they are plotted with high dpi (8000 to 20,000 dpi) plotting machines. In this case we used a transparent sheet mask only. The Figure 4.1 below illustrates the transparent sheet mask. The yellow color area in the design is left transparent so that only that part is exposed and rest filled section will not be exposed.

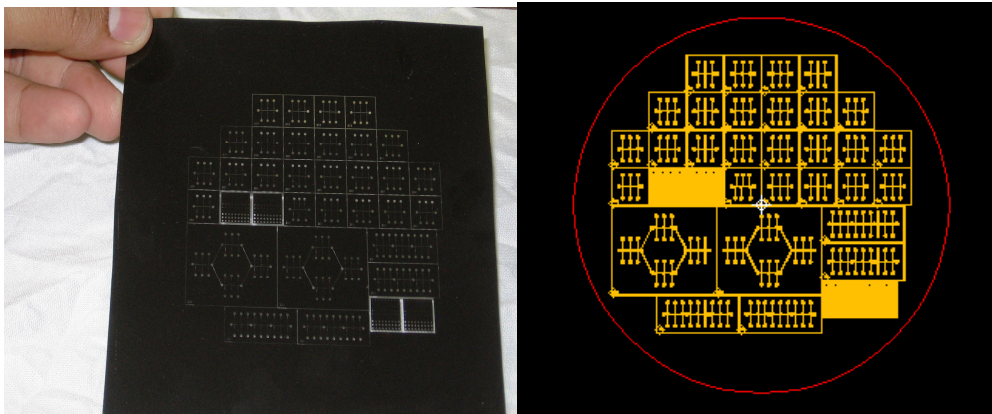




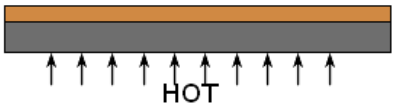
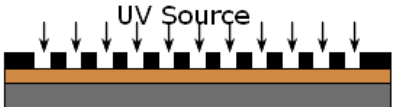
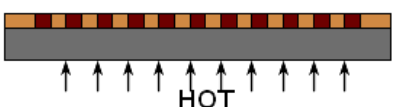
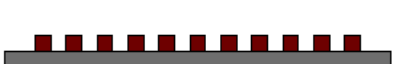
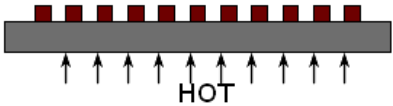

Figure 4.1: Transparency Sheet Printed Mask & Design Layout

#### 4.2.2 SU8 Master Mold Fabrication

The master mold fabrication involves *photolithography* process of thick SU8 photoresist. The SU-8 is a negative tone, epoxy-type, near-UV photoresist (365 nm) [32]. It is most popular in the field of Microfluidics due to its high cross-linking, chemical and thermal stability, low Young's modulus and easy to fabricate features with high aspect ratio structures (20:1), near vertical walls & 3d stacked structures. In this case, SU8-100 (*MicroChem Corp.*, USA) photoresist is selected to fabricate the mold for high aspect ratio channels of 10: 1.

The process involved in photolithography process is tabulated with graphical representations in table 4.1, followed by detailed process explanation.

Table 4.1: Master mold fabrication using photolithography process.

<i>Master Mold Fabrication Process</i>		
1	Dehydrated Si Wafer.	
2	Spin Coat SU8: 3000rpm @ 30sec.	
3	Pre Bake (PB): PB1: 65°C @ 10min. PB2: 95°C @ 30min.	
4	UV Exposure @ 60sec.	
5	Post Expose Bake (PEB): PEB 1: 65°C @ 1min. PEB 2: 95°C @ 10min.	
6	Developed with SU8 developer @ 7-10 min, followed by rinse with isopropyl and DI water.	
7	For additional cross linking, SU8 can be hard baked.	
		

*Wafer dehydrating* stage is the initial stage during photolithography process. This stage ensures the cleanliness and moisture content of the wafer that is used in photolithography process. If the wafers are not brand new then wafers are cleaned



depending upon the requirement. If minor contamination is observed on the wafer, then regular solvent cleaning by ultrasonication method or dilute acid dip will be fine. But if the contamination is high, then piranha etch cleaning will be better. Once the wafer is cleaned, then it is blow dried with nitrogen and further dehydrated at 200°C for 5min and then they are cooled down. In any case rapid cooling should be avoided. After dehydration the wafer is transferred for spin coating stage.

In *Spin Coating* stage the photoresist (SU8) is spread over the wafer using spin coater. By varying the spinning speed & spin time the photoresist thickness can be controlled. Spin speeds for different thickness of photoresist can be obtained from [33]. In our case to achieve 100µm thick film, the high viscous SU8-100 is static dispensed on to the wafer and spun at 3000rpm for 30 seconds. Once the spin coating of the photoresist is performed the wafer with photoresist is carefully removed from the chuck without any contamination and preceded to pre-bake process.

*Pre-exposure Baking or Soft Baking:* This process helps in evaporating the solvents in the photoresist and allows the photoresist to condense [33]. During this process the spin coated photoresist is baked in two stages. This improves the coating conformity and adhesion to the substrate [33]. The pre-exposure bake time varies with respect to thickness of photoresist. The suitable soft baking time can be obtained from the [33]. In our case the first pre-exposure bake is done at 65°C for 10 minutes and second pre-exposure bake is done at 95°C for 30 minutes. The baking can be done either using a furnace or a hot plate. In either case it is necessary to ensure that the photoresist is not rapidly cooled. Before proceeding to next stage it is important to ensure that the

photoresist is dry and non sticky towards the exposure side and also backside. Usually during wafer shifting from the spinner to hot plate or by using a contaminated tweezers, the backside of the wafer gets contaminated. This leads to failure in holding the wafer to mask aligner chuck. It can be avoided by wiping the backside of the wafer with solvent.

*Mask alignment & UV Exposure:* This stage is most critical for multiple layer exposure. In this case the design is based upon single layer technique. A Karl Suss MA56 mask aligner is used in this process. Initially the transparency sheet mask is attached to a transparent glass mask which is loaded on to mask holder on the aligner. Later the pre-baked wafer is loaded on to wafer chuck and then by aligning the mask with wafer they are exposed to a UV source of 365nm wavelength for duration of 60seconds, which provides about  $600\text{mJ}/\text{cm}^2$  of energy that helps in polymerization of the exposed photoresist. It is important to ensure the right exposure time. Improper exposure time leads to poor exposure or over exposure. In case of poor exposure the resist will not be able to polymerize completely and hence it releases from the wafer. By over exposure it might lead to shadow (finite area of particles next to the desired feature). Once the exposure is finished the wafer is released and post baked.

The *post exposure bake (PEB)* performed after the UV exposure helps in optimizing cross linking [33]. The PEB is also two stage process with different duration with respect to the thickness of photoresist. The duration for different thickness can be obtained from [33]. The PEB is done for shorter period compared to soft bake. In this case the first PEB is done at  $65^\circ\text{C}$  for 1minute and second PEB is done at  $95^\circ\text{C}$  for

10minutes. Once the PEB process is finished, the wafer is cooled to room temperature and developing process is implemented, followed by hard bake.

*Developing* of post baked SU8 wafer is performed by using a SU8 developer. Developing time varies with the thickness of the photoresist, with number of times the developer reused and agitation. A fresh developer will take 7-10 minutes to develop a 100 $\mu$ m thick photoresist. During developing the wafer should be completely immersed in the developer solution and continuously agitated through out the process. This agitation helps in developing properly. The developed wafer rinsed with isopropyl alcohol (IPA) and DI water followed by nitrogen blow drying. Once developing is finished the wafer is *hard baked* to increase the cross-linking and fidelity of SU 8 structure [33]. The hard baking is performed at 150°C – 200°C for about 15-20mins. The Figure 4.2 below illustrates developed wafer with SU8 pattern (master mold).

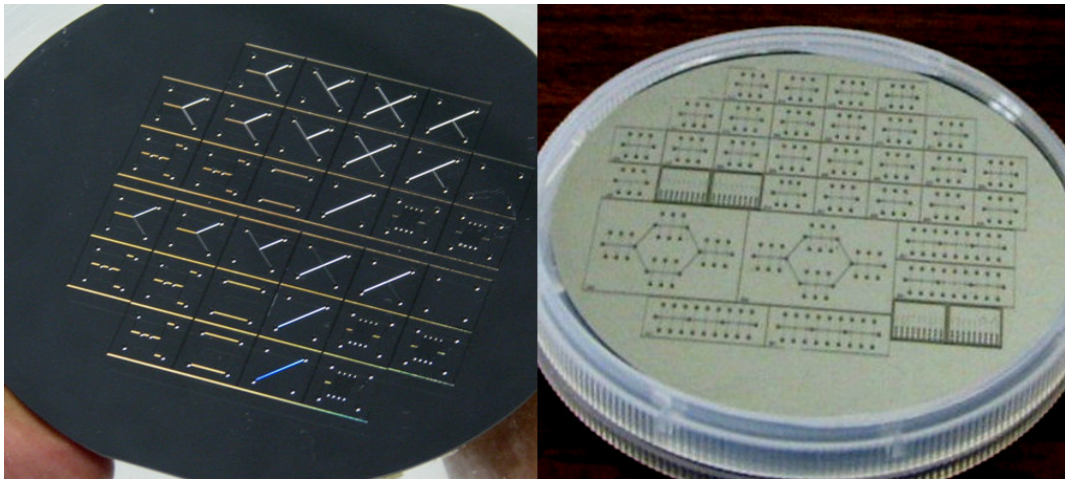


Figure 4.2: Developed master molds for different microfluidic circuits.

The developed SU8 master mold is profiled under *Veeco's Wyko NT1100 DMEMS optical profiler* (location *ARRI, UTA*) to ensure the developed thickness. The figure 4.3 illustrates thickness profile from the optical profiler scan, with an average thickness of  $100 \pm 5 \mu\text{m}$ .

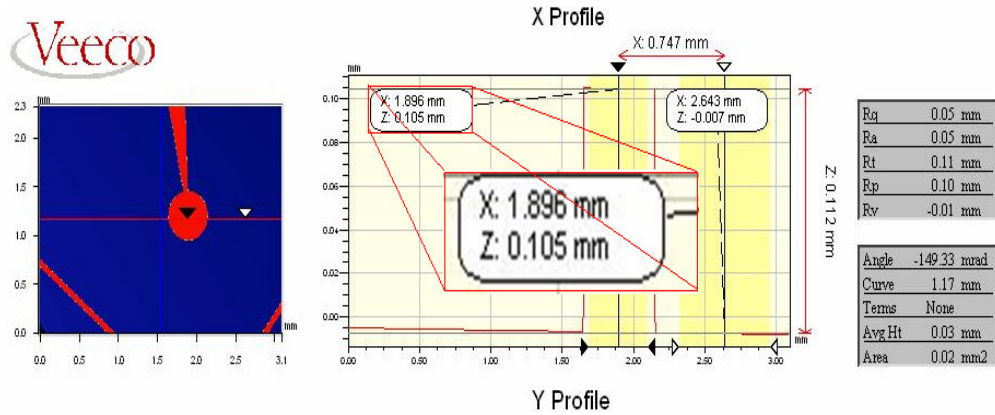


Figure 4.3: Optical profiling of SU8 master mold.

#### 4.2.3 Pattern transfer with replica molding

The master mold patterns are transferred on *polydimethylsiloxane* (PDMS) with replica molding [34]. The PDMS, a pre polymer which comes in two parts (silicon elastomer & a curing agent) is obtained from Dow Corning, USA. The pre polymer is mixed with curing agent depending upon the requirements (*i.e.*, *5:1*, *10:1*, *15:1*...). The change in mixture ratio will lead to change in young's modulus [35] and also helps in changing the stiffness of the material after curing. Hence flexible chips can be obtained by mixing with less curing agent. The mixture is degasified by placing it in a vacuum chamber to remove the air bubble formed during mixing. The Figure 4.4 clearly shows

need for degasification. The degasified mixture is dispensed on top of the SU 8 mold by placing it in a shallow container as shown in Figure 4.4.

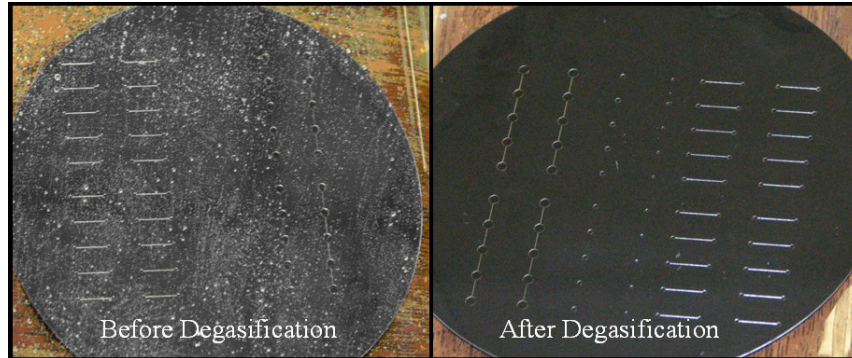


Figure 4.4: Before and after degasification of PDMS mixture.

The dispensed PDMS can be cured in two ways, room temperature curing and accelerated curing. Since the room temperature curing takes longer duration (1-2 days) depending upon mixture ratio, accelerated curing is performed by heating in a oven/ hot plate at 70°C - 85°C. By accelerated curing the PDMS can be fully cure in 20-30 minutes, depending upon type of mixture. The cured PDMS is then peeled carefully with out tearing. The Figure 4.5 below illustrates the peeling of PDMS and also the transferred pattern of the mold on PDMS.

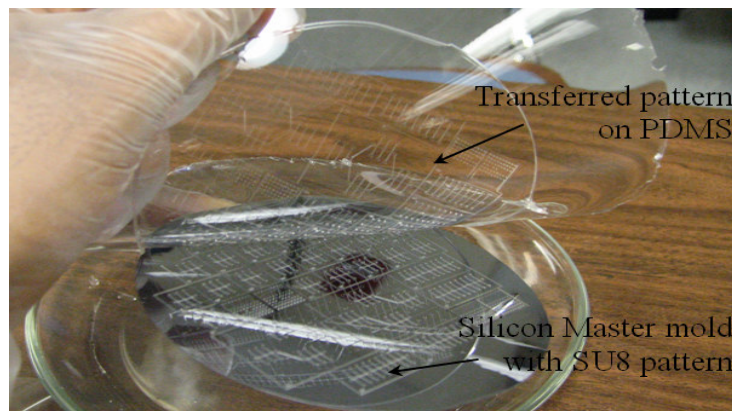


Figure 4.5: Transferred pattern on peeled PDMS.

#### 4.2.4 Fluidic interconnects & Bonding

Fluidic ports in PDMS are punched with a punch tool of diameter smaller than the outer diameter (OD) of the capillary tube that is to be inserted [36]. In this case we used a 0.5mm punch tool for capillary tubing with OD approximately 0.75mm to 1mm. The fluidic interconnects made in this technique were good even at 90psi. To avoid leakages, the fluidic interconnects can be sealed by applying excess PDMS around the capillary tubing in the end. Once the fluidic ports were punched, the wafer sized PDMS stamp is singulated in to individual dies. The singulated chips were sealed by bonding them with a plane PDMS layer or Pyrex glass slides. The bonding of PDMS to PDMS or Pyrex can be performed by oxygen plasma approach or semi-cured bonding approach. With plasma approach the surfaces that need to be bonded are activated under Oxygen Plasma. The bonding formed with this process is irreversible. The oxygen plasma treatment is done using a *Technics Micro RIE* at 145 -155mtorr of vacuum pressure with 20W of RF power at 10sccm of oxygen flow rate. The activated surfaces are brought in contact with gentle pressure followed by heat treatment at 100C for 10-15min. The heat treatment helps in improving the bond quality. The Figure 4.5 below illustrates a sealed PDMS chip with fluidic interconnects provided using the above process.

The semi-cure bonding is performed by placing the cured base chips on top of a semi cured plane PDMS layer and by full curing them. Even though semi-curing process does not involve any special equipment and cheaper when compared to plasma

bonding process, the overall bond quality differs and hence this limits the use of this approach.

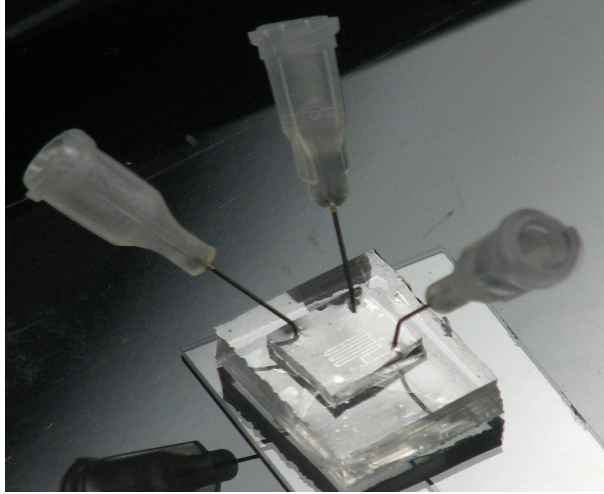


Figure 4.6: PDMS Microfluidic chip with fluidic interconnects.

### 4.3 Conclusion

The detailed fabrication process implemented in this research work is studied in this chapter with primary focus on PDMS based microfluidic circuits. The testing and analysis part of the fabricated samples are explained in the next chapter.

CHAPTER 5  
EXPERIMENTS & RESULTS

5.1 Introduction

This chapter provides the experimental results obtained from the PDMS microfluidic circuit and valve prototypes. The conducted experiments are bonding (1). Strength test of interconnects and sealing layer near the valve, (2). Deflection measurement of valve diaphragm, (3). Characterization of flow rate and pressure drop through the valve, and (4). Testing of flow direction control. The measured diaphragm deflection is compared to simulation result. The experiments and results discussed in this chapter are based upon die design 233 & 231 as in Figure 5.1, which consists of fluidic channel width  $50\mu\text{m}$ , membrane thickness of  $80\mu\text{m}$ , length of membrane  $600\mu\text{m}$  and  $400\mu\text{m}$  for die design 223.

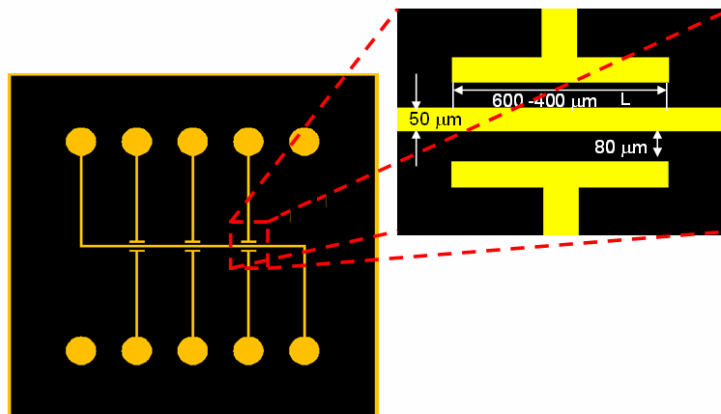


Figure 5.1: Die design 233(L =  $600\mu\text{m}$ ) & 231(L =  $400\mu\text{m}$ ).



## 5.2 Sealing layer & Interconnects Testing

The bonding strength of the sealing layer near the valve diaphragm plays a major role in the valve operation. Poor bond introduces air in to the channels, leading to valve function failure. Bonding strength of the sealing layer was tested by supplying pneumatic pressure into the valves. This test is to determine the maximum sustainable operating conditions for the designed valve and interconnects. As explained in the chapter 4, PDMS chips were fabricated with the two different bonding techniques, i.e. oxygen plasma process and semi-cured bonding. These samples are tested with pneumatic pressure 0 ~ 80psi.

Figure 5.2 shows the experimental setup for pressurizing test. The pneumatic pressure is regulated with a SMCT<sup>TM</sup> regulator for the valve operating pressure. A set of SMCT<sup>TM</sup> solenoid valves are attached to the regulated pneumatic source and the solenoids switch pneumatic pressure to the PDMS valve structure. The on/off switching action of solenoid are controlled by a driver circuit using UDN2981A (*Allegro's 8 channel source driver*). The configuration of valve pressurizing test is shown in figure 5.1.

The valve structures were operated with various pressure ranges with fluid inside the channel to locate the leakage during the bond failure. The figure 5.4 shows the leakage observed due to bond failure of the chips that were bonded with oxygen plasma treatment (145-155mtorr @ 20 W and heat treatment).

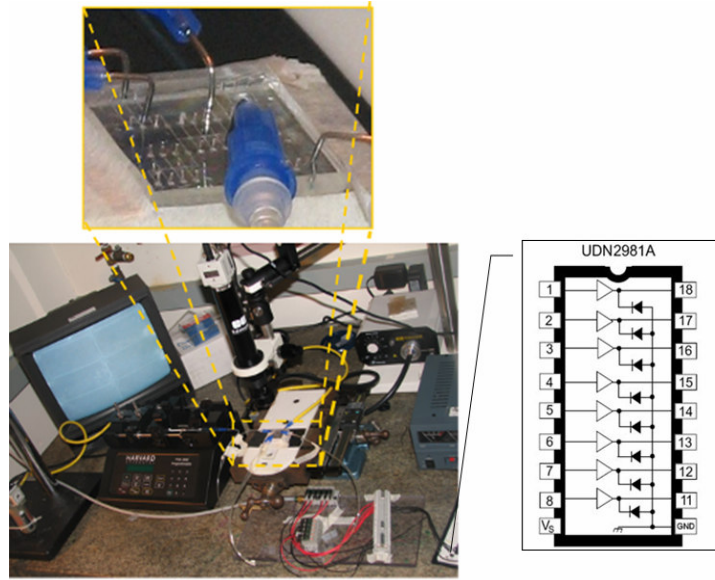


Figure 5.2: Photo of experimental setup for pressurizing test.

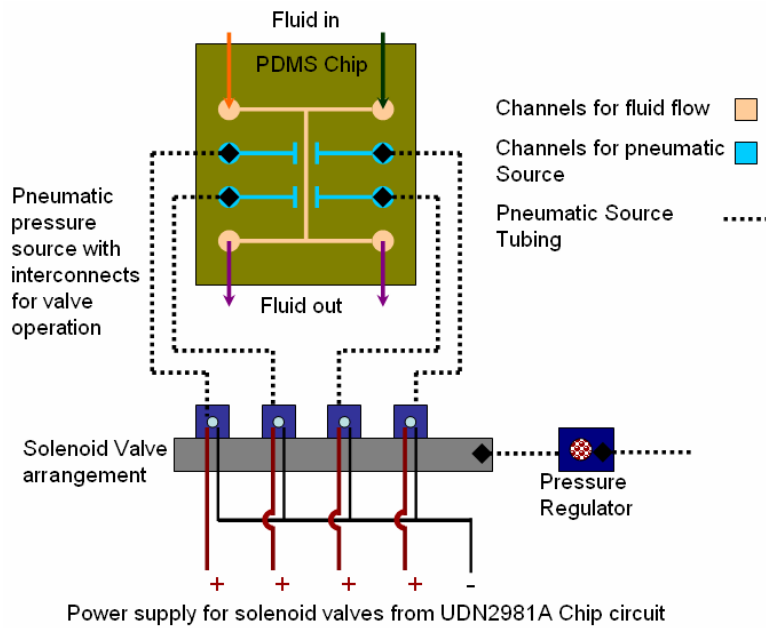


Figure 5.3: Configuration of valve pressurizing test.

The dimensions of the diaphragm and the channel can be observed in the figure 5.4 (a). These valves were able to hold pressure up to 80psi. The deflection of the

diaphragm at this pressure can be observed in figure 5.4(b). Once the bond fails, the high pressure air flushes the fluid from the channels. The leakage developed due to bond failure is also effective even at low pressure ranges. The failed chip was retested with low pressure, and figure 5.4 (c) shows bubble formation from the air leakage. This test was repeated to ensure the bond failure. In most cases the bond failure has occurred in between 70psi to 80psi.

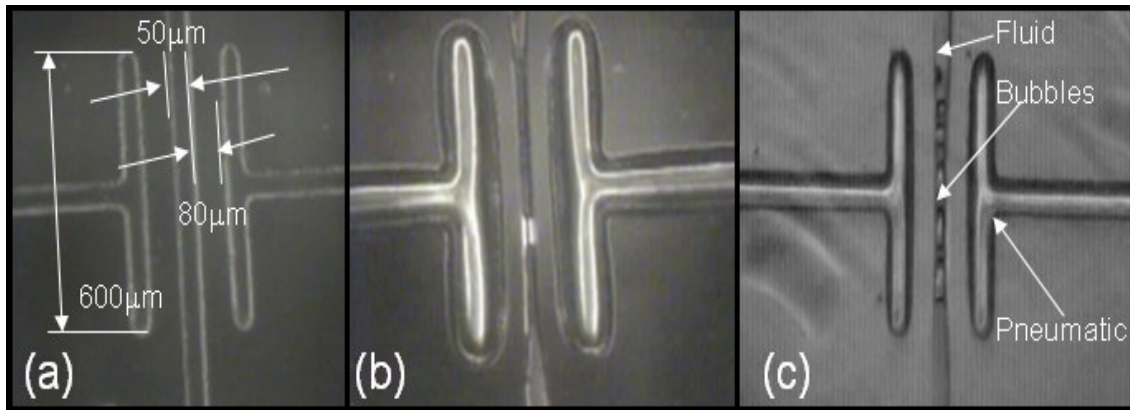


Figure 5.4: Top view of valve during sealing layer testing (a) valve at 0psi, (b) valve at 80psi, & (c) valve at 30psi.

The bonding strength with oxygen plasma treatment was stronger than the bonding with semi-cured PDMS base layer. For the bonding with semi-cured PDMS the die needs to be placed gently upon the semi-cured PDMS layer so that it won't allow any air to trap in between and lead to fail the bond. From figure 5.5, it can be observed that the bond is not clear, and hence due to the air trap the bond failed. In most cases the bonding was not successful due to air trap and poor bonding conditions. The bond

failure from semi-cured process can be observed in figure 5.5. Due to the bond failure in all samples, valve functional test was not implemented.

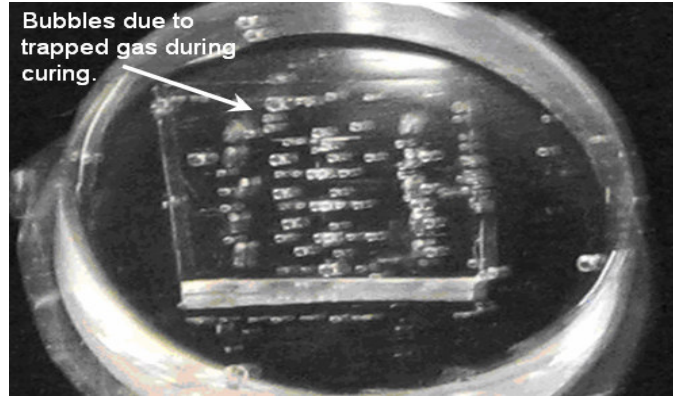


Figure 5.5: Trapped gas in a PDMS chip bonded with semi-cured bonding process.

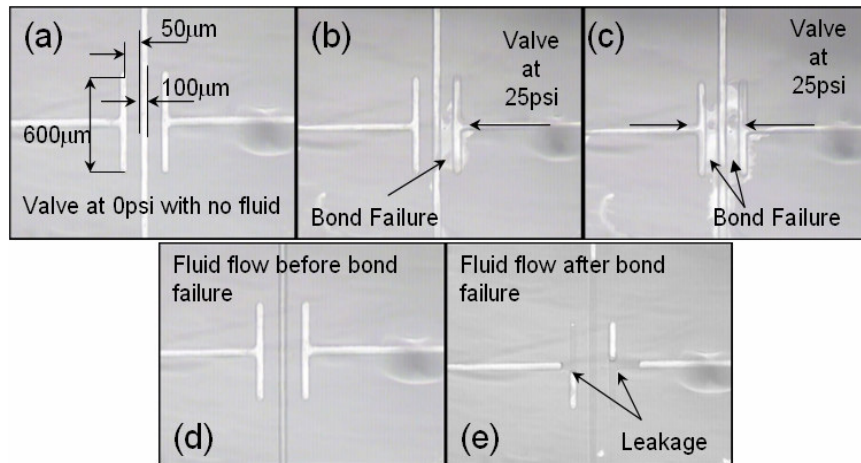


Figure 5.6: Testing of PDMS chip bonded with semi-cured bonding process: (a) open valve, (b) single side initiated valve, (c) double side initiated valve, (d) fluid flow before bond failure & (e) fluid flow after bond failure.

Interconnects provided to the chip are of press-fit type with a 22 gauge precession stainless steel tip (*EFD Inc.*) inserted into a punched hole of 500µm. The figure 5.7 illustrates the press fit interconnects used in testing. Through out the testing

process for bonding evaluation, interconnects were firm till a maximum pressure of 80psi. In some cases when the punched hole is not clear interconnects leaked and failed.

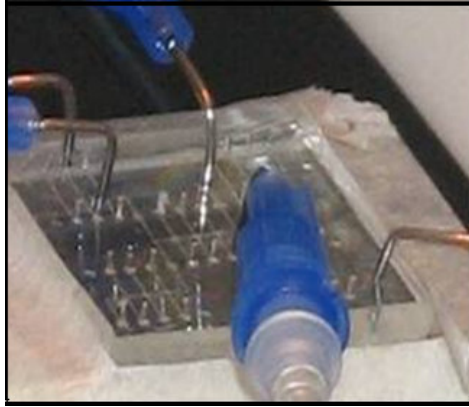


Figure 5.7: Precession stainless steel interconnects.

### 5.3 Valve diaphragm deflection test

The verification of embedded in-plane valve diaphragm displacement is observed in this section. The valve is subjected to pressure range from 0psi to 80psi. The valve diaphragm deflection is observed with a zoomed CCD camera and the deflection is calculated by pixel counting from the captured image. The figure 5.8 illustrates the deflection of valve membrane at various operating pressures. In figure 5.9, graphical illustration for comparison between the deflections measured and ANSYS simulation are observed. As explained in [30] about the improved flexibility with different mixture ratio of the PDMS, the simulation result obtained for the different PDMS mixture ratio is observed in the figure 5.9. The maximum required pressure to close the channel was 65psi for the valve of 400 $\mu$ m of diaphragm length, 50 $\mu$ m of diaphragm width and 80 $\mu$ m of channel width.

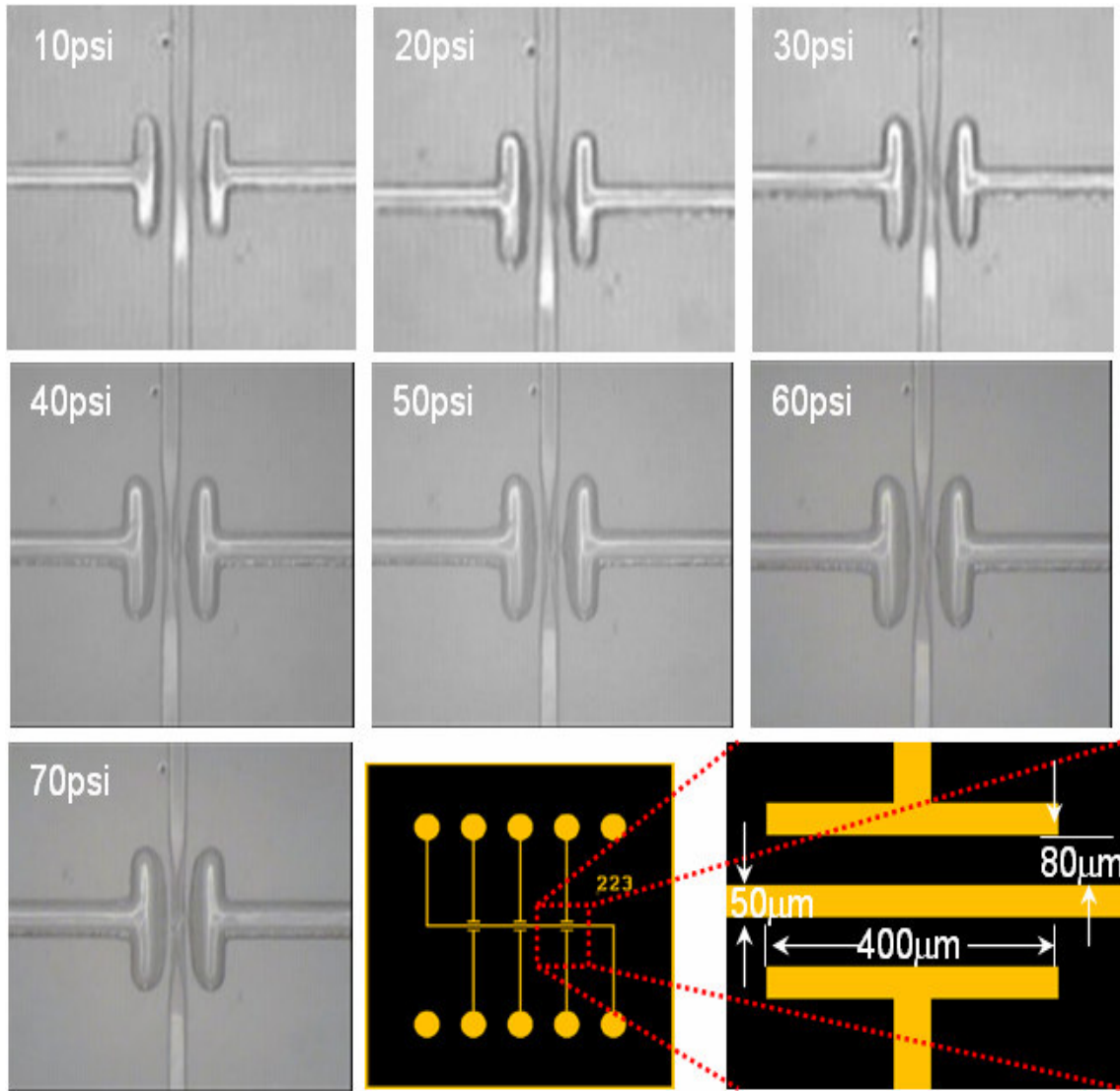


Figure 5.8: Deflecting valve membrane at various pressures.

Table 5.1: Change in young's modulus with respect to PDMS mixture ratio [30]

PDMS Mixture	Young's Modulus (M Pa)
10:1	0.75
15:1	0.36

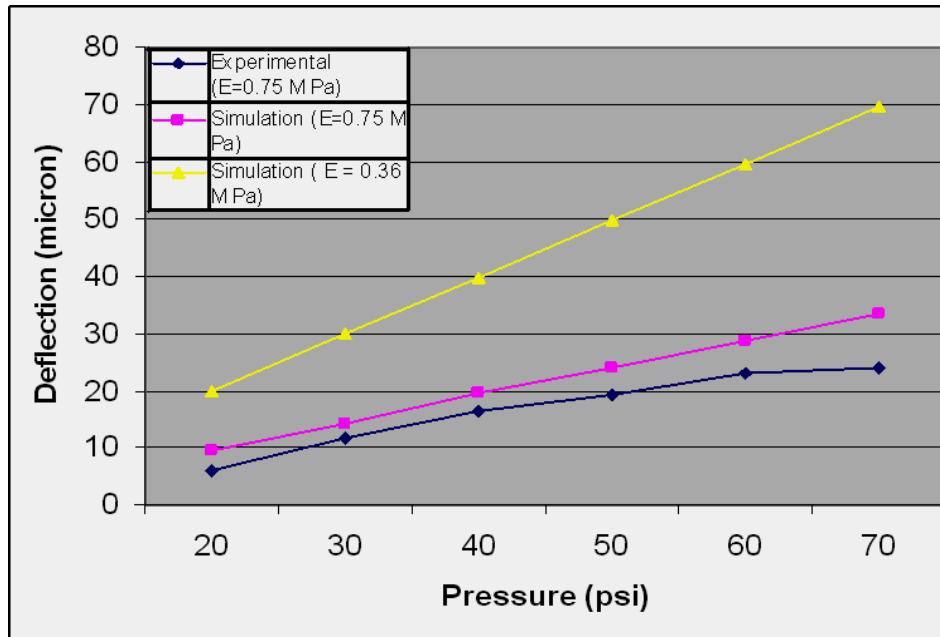


Figure 5.9: Graphical illustration of *deflection Vs pressure*.

#### 5.4 Functionality Test

This section discusses about the functionality and evaluation of the reconfigurable chip.

The chips with embedded in-plane valves is designed to provide basic functions like flow (on/off) control & direction control. The chip that was used for this functional verification is shown in figure 5.10. The leakage was measured by calculating the flow rates with valve at turn on and off. The schematic of the leakage testing setup is seen in figure 5.11. The fluid was driven through a dispensing syringe with the help of a constant pneumatic source of 10psi pumping and the flow rate was measured with the valve turned on and off. The table 5.2 provides with the flow rate data.

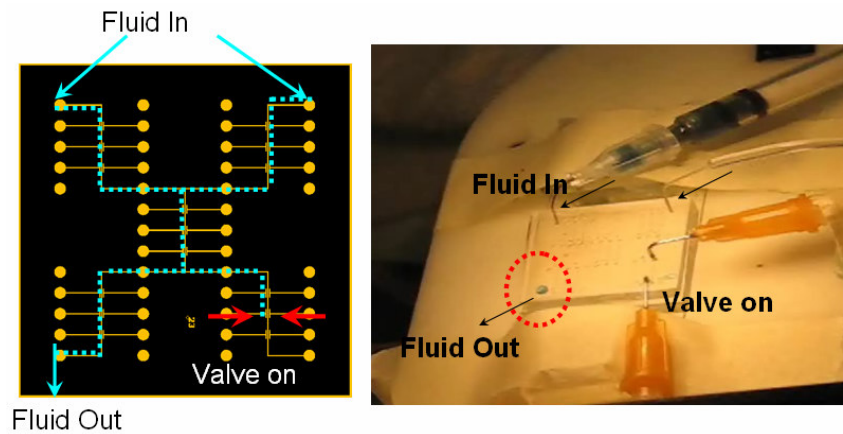


Figure: 5.10: Illustration of direction control fluid flow.

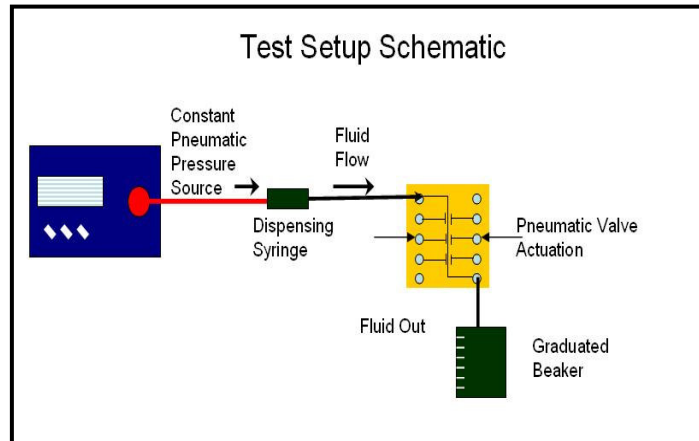


Figure 5.11: Schematic of leakage testing setup.

The fluid was driven through a dispensing syringe with the help of a constant pneumatic source of 8psi pumping and the flow rate was measured with the valve turned on and off. The table 5.2 provides with the flow rate data. The die used for this test has a 400 $\mu\text{m}$  diaphragm length, 50 $\mu\text{m}$  diaphragm width and 80 $\mu\text{m}$  of channel width. The valve was operated at two peak pressures and the flow rate obtained as observed as in the table.



Table 5.2: Measured flow rate at two peak operating pressures.

Flow rate measurement with valves at different operating pressure and constant inlet pressure at 8psi		Valve actuation pressure		
		0 psi	60psi	70psi
Flow rate ml/min	Die 223	85.714	50.847	40.013
	Die 223	83.333	48.387	37.500
	Die 223	92.308	54.545	41.379

### 5.5. Conclusion

This chapter explained tests conducted to verify the chips functionality. The chips used in this test are of two types, where they defer from each other in diaphragm length. The chip has a leakage ratio between 0.4 to 0.2, which can be observed from the flow rate table. The chip is able to perform direction control flow for a short period time, due to the leakage noticed over a period of time.

## CHAPTER 6

### CONCLUSION & FUTURE WORK

#### 6.1 Conclusions

The simulation and experimental results show that the membrane deflects up to  $25\mu\text{m}$  at 70psi in  $100\mu\text{m}$  (height)  $\times$   $50\mu\text{m}$  (width) channels. The chip has a leakage ratio ranging between 0.4 - 0.2, which can be observed from the flow rate table. The chip is able to perform direction control flow for a short period time, due to the leakage noticed over a period of time. The pressure required to close the channel can be lowered by selection of suitable material properties and channel dimensions. To minimize the operating pressure, design modifications with reduced membrane and channel width, and reduction of material stiffness by changing mixture compositions are being evaluated. Embedded, in-plane valves facilitate fabrication of microfluidic systems with improved volume metering and directional control for discrete volume manipulation.

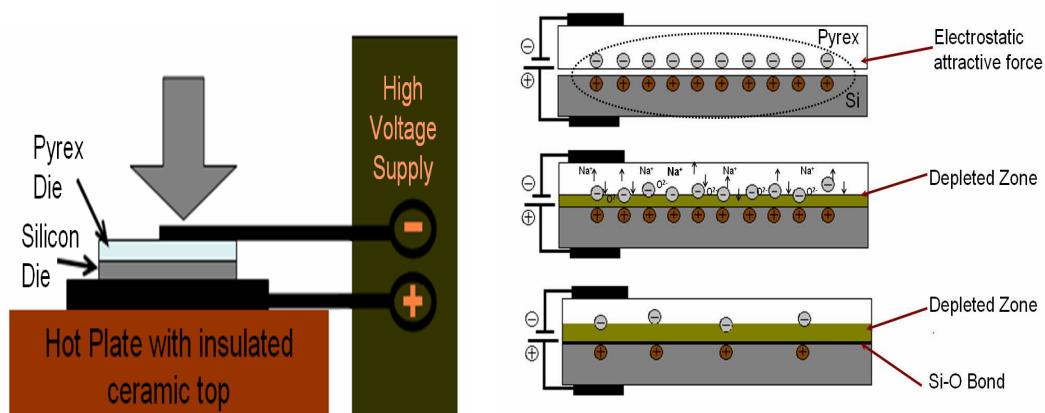
#### 6.2 Future Work

A complete valve characterization with different PDMS mixture ratios can be performed to improve the valve efficiency. Testing of the modified designs shown in appendix for different valve arrangements which provide multiplexing, mixing, and single sided valve configuration with mixing and diverging need to be performed. Contact element analysis for the deflecting membrane helps in further design modifications.

## APPENDIX A

### ANODIC BONDING OF SI & PYREX GLASS DIES

The anodic bonding process makes permanent hermetic sealing (bonding) between Silicon wafer & Pyrex glass wafer, below the softening point of the glass under electric field. It is an example for Field Assisted Bonding [37]. At elevated temperature & high voltage condition, the sodium ions migrate from the interface by depleting the interface. The resulting electrostatic attraction brings the Si & glass into intimate contact. With this, oxygen anions flow towards the silicon from glass with anodic reaction in between them, which leads to a permanent chemical bond with silicon. The following figure illustrates anodic bonding process & setup.



Schematic illustration of Anodic Bonding of Pyrex & Silicon wafers setup & process.

The detailed bonding procedure involves:

- i. The two dies (Pyrex & silicon) were properly cleaned by ultrasonic solvent bath and rinsed with DI water and dried by blowing Nitrogen gas.

- ii. The two dies were placed on aluminum base plate, which is located on top of the hotplate and then aligned with the help of available optical setups (stereo dynascope).
- iii. After the alignment process, the top probe (negative end in the circuit) is brought down carefully to apply gentle pressure on the top die and to maintain the die intact with the bottom die.
- iv. Now the dies were heated to 450°C and maintained at the same through out the process on the hotplate.
- v. Once the hotplate reaches the required temperature, high DC Voltage of 1KV is supplied with gradually increment and maintained at this condition till 10-14 minutes to finish the bonding process.
- vi. Meanwhile to ensure the process is not shorted, the current flow and voltage were monitored. The figure 4.4 below illustrates of the current flow with respect to time obtained from the monitored readings show in table 4.1.
- vii. Once the bonding is done, turn off the voltage to zero with gradual decrement in voltage and turn off the hot plate.

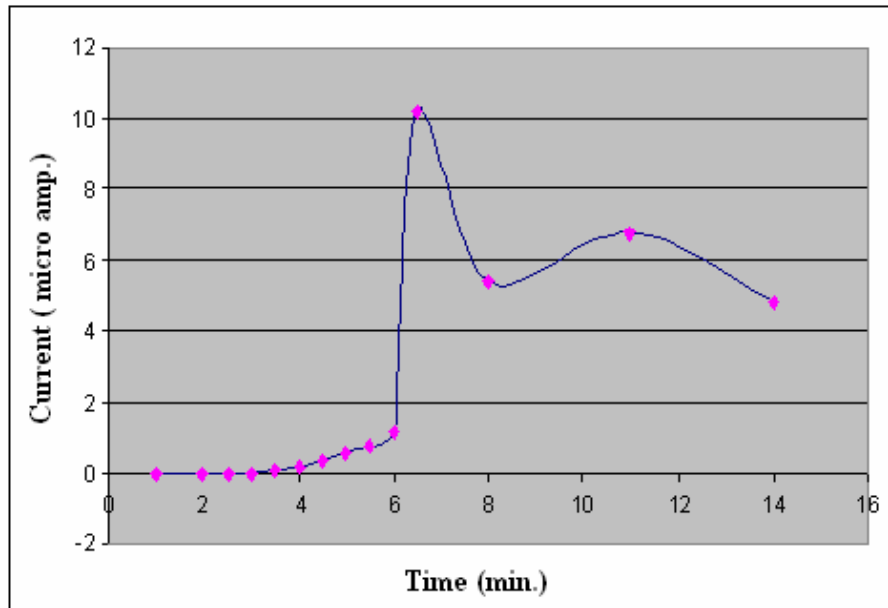


Illustration of Current flow monitored during bonding process.

Even though the estimated bonding process time 10-14 min been reported in many research articles. Based upon our laboratory setup, the bonding process is been monitored and hence the results were obtained.

APPENDIX B

MICRO DRILLING SETUP

The ports for Microfluidic interconnects can be fabricated using various techniques like Anisotropic Etching, Non-conventional Drilling, and Conventional drilling etc... In this case we used a lab based Microdrilling stage (conventional technique), with electroplated diamond tip drill bits. The drilling is performed at higher spindle speeds with very low feed rate. The microdrilling stage consists of three parts. The first is microdrilling assembly, which is a standard high speed handset carving drill attached to a manual/ semi automatic Z micromanipulator with a customized aluminum fixture, which can be moved by DC voltage source with a DPDT switch to change the polarity during the feed or use a motion controller set for the motorized z- stage. The drill (Ram Products Inc., USA) accepts a different drill-bit shank sizes with different collets extension for different drill bits (1/8, 1/16, 1/32 inch) and has a variable speed control up to 45,000 rpm. Drill bits are composed of Diamond Core with range of diameters from .001" to 48" (UKAM Industries, USA). The second is a standard rectangular stage with X-Y manual controls, where sample rests during the drilling process. The third part is the visual inspection part, which is a high resolution, high focus camera which is attached to the display unit next to the stage for quality visual inspection during the process. The combination of the X-Y and Z micromanipulators stage permit precise placement of the micro drill and sample. The figures (1 & 2) below illustrates the drilled holes images, drill bits & micro drilling stage



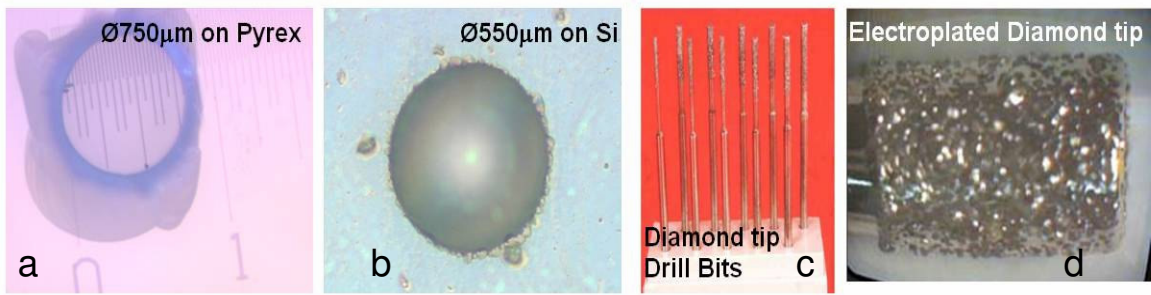


Figure 1: a & b Drilled holes, c & d diamond tip drill bits (source: *Ukam Industries, USA*)

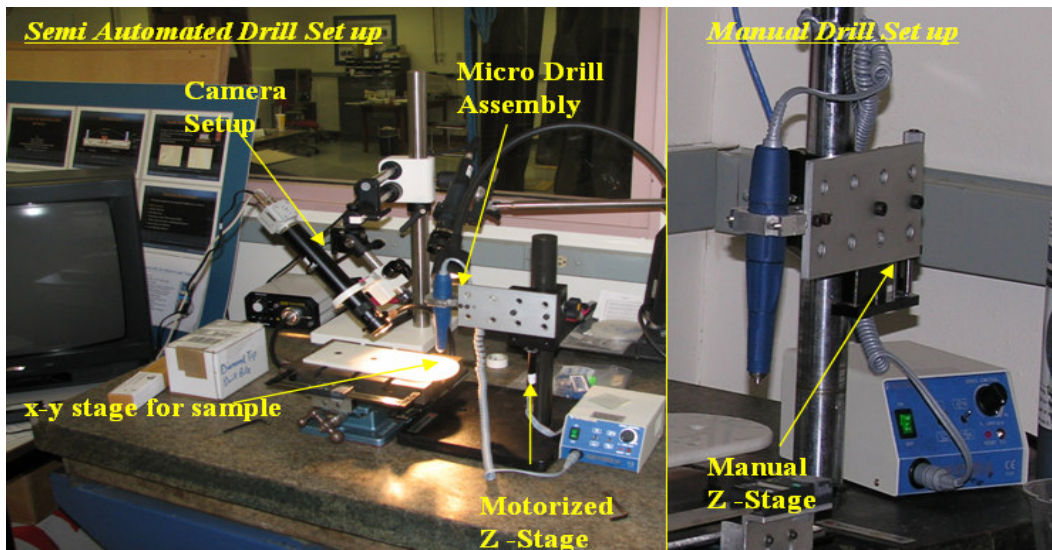
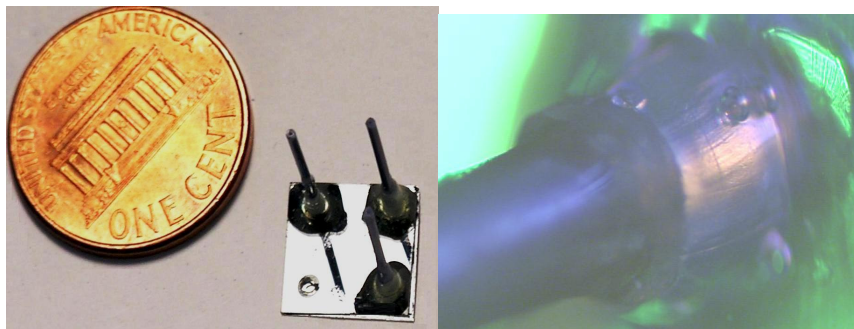


Figure 2: Microdrilling stage, components & drilled holes

## APPENDIX C

### EPOXY BASED FLUIDIC INTERCONNECTS

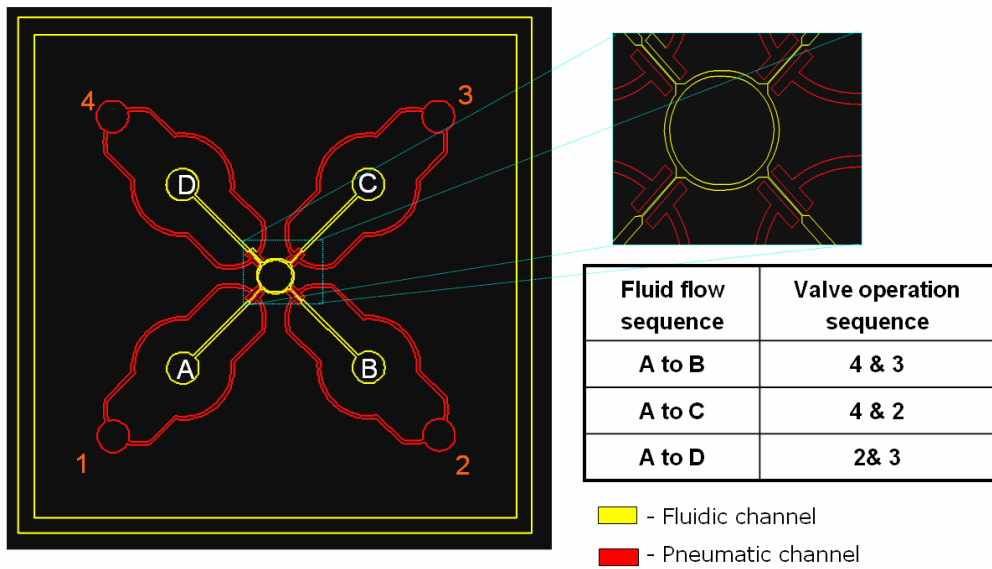
The fluidic interconnections were made with the help of drilled ports and capillary tubing (Up Church scientific). The capillary tubing is initially capped with short length tubing with its inner diameter close to the outer diameter of the capillary tubing. The capped tubing is glued to the capillary tubing and then it is inserted in to the fluidic port. While inserting the capillary tubing into the fluidic port, the capped tubing allows us to control the insertion length. Later by applying reasonable amount of epoxy on top of the inserted tubing we can provide fluidic interconnection to the chip/ die. But during the process of applying epoxy on top, usually it messes up and slides into the channel and clogs the channel. This channel clogging problem can be avoided by applying gentle pressure from top on the capillary tubing, which locks the port with the capped tubing. From the figure below, Microfluidic chip with interconnections and cross section schematic of interconnection can be observed.



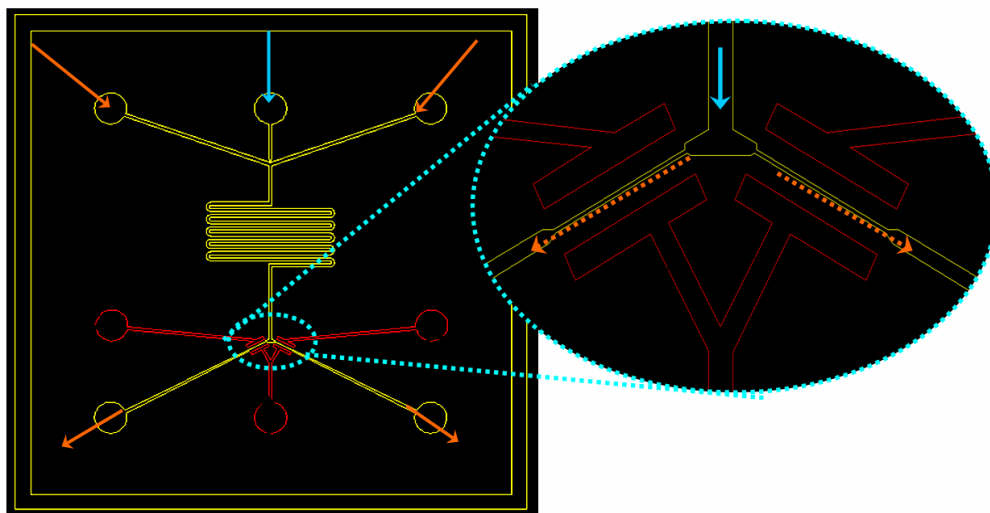
Photograph of Epoxy based Fluidic Interconnection

## APPENDIX D

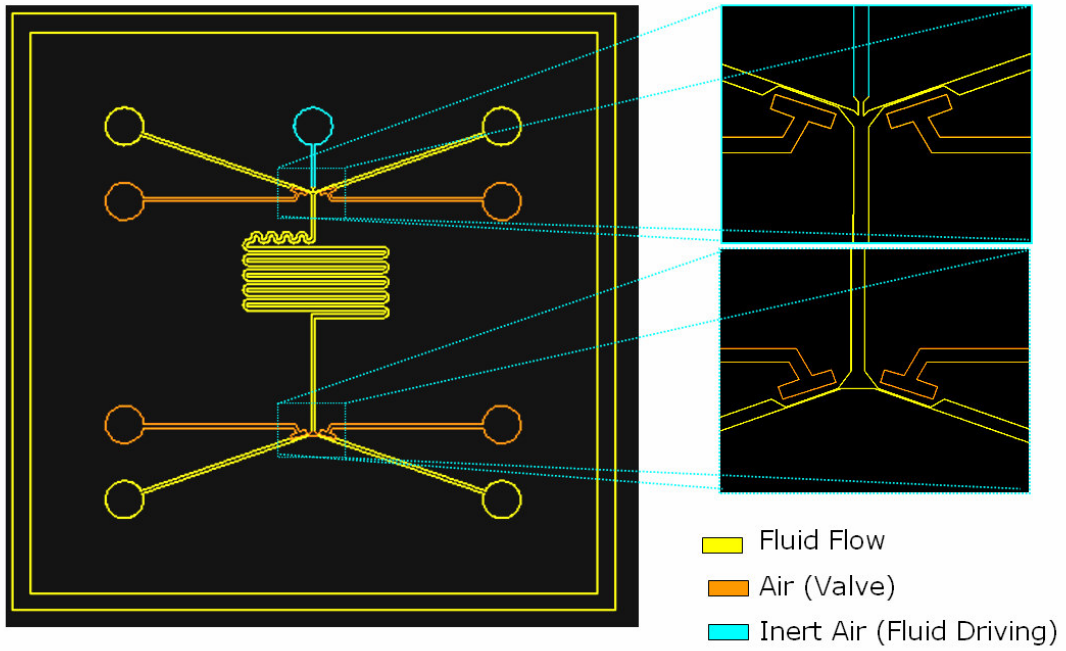
### MODIFIED MICROFLUIDIC CIRCUIT DESIGNS



Multiplexing Microfluidic circuit with embedded in-plane valve



Mixing and diverging circuit with embedded in-plane valve.



Mixing and diverging circuit with embedded in-plane valve (single side).

## REFERENCES

1. S. Terry, J.H. Jerman, J. Angell, "A gas chromatographic air analyzer on a silicon wafer", *IEEE Trans. Electron. Devices*, ED-26, 1880 (1979).
2. D. Reyes, D. Iossifidis, P-A. Auroux, A. Manz, *Anal. Chem.*, 74, 2623 (2002).
3. A. Manz, N. Garber, H.M. Widmer, "Miniaturized total chemical analysis system: a novel concept for chemical sensing", *Sens. Actuators*, 1990, B1, 244-248
4. Patrick Tabeling, "*Introduction to Microfluidics*", Oxford press, UK; ISBN 0-19-856864-9.
5. Roland Zengerle and Hermann Sandmaier, "*Microfluidics in Europe*", *AIAA- 97*, 1788.
6. C.G.J. Schabmuller, M. Koch, A.G.R. Evan and A. Brunnschweiler, "Design and fabrication of a microfluidic circuitboard", *J. Micromec. Microeng.* 9(1999) 176-179.
7. K. A. Shaikh, et al., "A modular microfluidic architecture for integrated biochemical analysis", *PNAS*, July 12, 2005, vol. 102, no. 28, 9745–9750.
8. B. Xu, K.T. Ooi, C. Mavriplis and M.E. Zaghoul, "Viscous dissipation effects for liquid flow in microchannels", *Nanotech 2002 Vol. 1*, 100 – 103.
9. Young-Min Kim, Woo-Seung Kim, Sang-Hoon Lee & Ju-Yeoul Baek, "Effects of Surface Roughness on the Flow Characteristics in PDMS Microchannels",

- Microtech. in Medicine and Biology, 2005. 3rd IEEE/EMBS, 12 May 2005, 292-295.
10. Eui-Hyeok Yang and David Bame of Caltech for NASA's Jet Propulsion Laboratory.
  11. Zheng Cui, "A Knowledge Base for Microfluidic Devices", Rutherford Appleton Laboratory, UK.
  12. S.Shoji, M.Esashi and M.marsuo, "Prototype miniature blood gas analyzer fabricated on a silicon wafer", *Sensors and Actuators*, 14, 101-107 (1988).
  13. M.A.Huff, J.R.Gilbert and M.A.Schmidt, "Flow characteristics of a pressure-balanced microvalve", *Tech. Dig. of Transducers'93*, 98-101 (1993).
  14. T. Ohnstein, et al., "Micromachined silicon microvalve", *Proc. IEEE MEMS*, pp. 95-98 (IEEE, Piscataway, NJ: 1990).
  15. P.W.Barth, "Siliconmicrovalves for gas flow control", *Tech. Dig. Transducers'95*, V.2, 276-279 (1995).
  16. E. Carlen and C. Mastrangelo, "Paraffin actuated surface micromachined valves." U. Michigan (2000).
  17. K.Yanagisawa, H.Kuwano and A.Tapo, "An electromagneticall driven microvalve", *Tech. Dig. Transducers'93*, 102-105 (1993).
  18. Marc A. Unger, et al, "Monolithic microfabricated valves and pumps by multilayer soft lithography", *Science*, April 2000, Vol. 288 .
  19. William H.G., et al, "Development and multiplexed control of latching pneumatic valves using microfluidic logical structures", *Lab Chip*, 2006, 6, 623-631.



20. T. Vestad, D.W.M. Marr and J. Oakey, "Flow control for capillary-pumped microfluidic systems", *J. Micromech. Microeng.*, 14 (2004), 1503–1506.
21. Saket Karajgikar, "Microfluidic interconnections – literature overview", internal technical report, ARRI, UT Arlington, summer 2006.
22. Yao T. J., Lee S., Fang W. and Tai Y. C., "Micromachined Rubber O-ring Micro-Fluidic Couplers", *MEMS*, 13<sup>th</sup> Annual International Conference, Jan-2000, Page(s):624 – 627.
23. Aniruddha Puntambekar and Chong H Ahn, "Self-aligning microfluidic interconnects for glass- and plastic-based Microfluidic systems," *J. Micromech. Microeng.* 12 (2002) 35–40.
24. Li S. and Chen S., "Polydimethylsioxane Fluidic Interconnects for Microfluidic Systems," *IEEE TRANSACTIONS ON ADVANCED PACKAGING*, VOL. 26, NO. 3, AUGUST 2003.
25. Gray, B.L., Collins S. D. and Smith R., L., "Interlocking mechanical and fluidic interconnections for microfluidic circuit boards," *Sensors and Actuators A* 112 (2004) 18–24.
26. Tsai H. and Lin L., "Micro-to-macro fluidic interconnectors with an integrated polymer sealant," *J. Micromech. Microeng.* 11 (2001) 577–581
27. Samuel K. Sia and George M. Whitesides; "Review: Microfluidic devices fabricated in poly (dimethylsiloxane) for biological studies", *Electrophoresis* 2003, 24, 3563-3576.

28. Kazuo Hosokawa and Ryutaro Maeda; “*A pneumatically-actuated three-way microvalve fabricated with polydimethylsiloxane using the membrane transfer technique*”. *J. Micromech. Microeng.* 10 (2000) 415–420.
29. Yang X, Grosjean C, Tai Y C and Ho C M; “*A MEMS thermopneumatic silicone rubber membrane valve*” *Sensors and Actuators, A* 64 (1998) 101-108.
30. Armani, D. Liu, C. Aluru, N. “*Re-configurable fluid circuits by PDMS elastomer micromachining*”, *Micro Electro Mechanical Systems, 1999. MEMS '99. Twelfth IEEE International Conference, 17-21 Jan 1999, Orlando, USA.*
31. J.A. Rogers, & R.G. Nuzzo, “Recent progress in soft lithography”, *Materials today*, 8, 2005, 50 – 56.
32. Louis J. Guerin “THE SU8 HOMEPAGE” - by
33. NANO™ SU-8: Negative Tone Photoresist Formulations 50-100., Microchem Corp., USA
34. Younan Xia and George M. Whitesides; “Review: Soft Lithography”, *Annu. Rev. Mater. Sci.* 1998. 28:153–84.
35. Deniz Armani, Chang Liu and Narayan Aluru; “Re-configurable Fluid Circuits by PDMS Elastomer Micromachining”, *MEMS, 12<sup>th</sup> IEEE International Conference, Orlando, FL, USA 1999.*
36. Andrew M Christensen, David A Chang-Yen and Bruce K Gale; “Characterization of interconnects used in PDMS microfluidic systems”, *J. Micromech. Microeng.* 15 (2005) 928–934

37. Kevin B. Albaugh & Paul E. Cade; "Mechanisms of anodic bonding of silicon to pyrex glass", 1988 Solid State Sensor and Actuator Workshop. Technical Digest (Cat. No.88TH0215-4)

## BIOGRAPHICAL INFORMATION

Srikar Paruchuri received Bachelor's degree in Mechanical Engineering from Jawaharlal Nehru Technological University, Hyderabad, India. His research interests are design, fabrication and packaging of Micro & Nano Scale Devices in various fields like Bio-Sensing, Photonics, Thermal Cooling etc.,. He attended TheUniversity of Texas at Arlington for Master of Science degree in Mechanical Engineering Department. At UTA he joined Prof. Dereje Agonafer's Electronics MEMS & Nanoelectronics Systems Packaging Center, where he started working in Microfluidic Packaging. He received graduate research assistantship at Automation & Robotics Research Institute (ARRI) in summer 2005 and worked with multi-disciplinary research team till fall 2006 and as a part of research he gained hands on experience in micro fabrication and packaging techniques. Apart from his experiences in United States he had undergraduate work experience, internship experience at Electronics Corp. of India Ltd and co-op at Central Institute of Tool Design both located in Hyderabad, India.